Bears, berries, bearings on the landscape: Monitoring American black bear (Ursus americanus) populations, habitat use, and movements in Idaho

A Thesis

Presented in Partial Fulfillment of the Requirements for the

Degree of Master of Science

with a

Major in Natural Resources

in the

College of Graduate Studies

University of Idaho

by

J. Matthew Nelson

Approved by:

Major Professor: David Ausband, Ph.D.

Committee Members: Janet Rachlow, Ph.D.; Sophie Gilbert, Ph.D.; Shane Roberts, Ph.D.

Department Administrator: Lisette Waits, Ph.D.

December 2022

Abstract

Black bears populations have historically been managed using harvest data and mark-recapture methods. New methods such as the time to event and space to event models have opted to estimate unmarked populations using trail cameras and have so far been tested on high density ungulate species and low density carnivore species.

In the first chapter, we apply these two models to estimating black bear populations in several study areas across Idaho. Black bears represent an optimal species to test these models because they occur at a medium density between most carnivores and ungulates and have different movement patterns and life histories. We tested the efficacy of these models by comparing the resulting densities to comparable black bear densities found throughout similar habitats. We found that while the models did sometimes find comparable density estimates, they were often dependent upon camera placement style and the time to event model tended to overestimate populations frequently. Incorporating bootstrapping worked to bring some estimates into the comparable density range (particularly with time to event), but still resulted in high estimates. Bootstrapping the space to event model, however, often biased estimates quite low, presenting an issue where bootstrapping the models was not always the best course of action.

Black bear recruitment in Idaho is strongly correlated with the late summer huckleberry crop, with low crops affecting fall black bear weights and the capability to successfully reproduce. In chapter two, we attempted to create a model predicting the huckleberry crop for the upcoming year so that managers could have a preemptive tool for managing black bear populations. Models for 2020 and 2021 found that there was some overlap in predictive covariates for huckleberry productivity, but several additional covariates were included in 2021. We also did not find a strong correlation between our 2020 model and black bear recruitment for the following year, possibly due to the short duration of our study.

Acknowledgements

The Idaho Department of Fish and Game funded this project and conducted the photo analysis for the St. Joe and Clearwater study areas in 2020 and 2021. A big thank you to Sarah Thompson for her help with all things camera related and for making sure 500 cameras worth of data was organized and easy to work with. Thank you to the regional staff at the Coeur d'Alene, Lewiston, and McCall offices for their help with logistics and gear. Black bear trapping is a huge undertaking, particularly for someone who had never trapped bears before. Thank you to Jeremy Nicholson for making the trip all the way from Idaho Falls to train myself and the crew and set up our first trapline; I hope the morels were a worthy compensation. Also thank you to Jim Hayden for spending his last week before retirement training us in the field and taking a bottle of ten-year old blood to the face. A huge thanks to John Beecham and Jeff Rohlman for spending several weeks camping in Council deploying collars. It was truly a pleasure to learn from and experience trapping with two of the greats.

Thank you to my committee: Dr. Janet Rachlow, Dr. Sophie Gilbert, Dr. Shane Roberts, and Barb Moore. You were invaluable to guiding me through this project and graduate school. Dr. Dave Ausband, you took a chance on me and helped to show me what research is (it all begins with the qhp's). You were there with both professional and personal guidance and pushed me to be the best biologist I could be; I could not have asked for a better advisor and mentor. Going forward, I will always make sure to both ask questions and for help.

This project required a considerable amount of field work and data collection. Thank you to my four crew leads throughout the years: Kat Petersen, Meghan Diamond, Leon Burman, and Brooks Pitman. You all put in way more than expected into this project and were invaluable in keeping me organized. To the three years of field crews, thank you for the long hours, miles, bushwhacking, and days without bathing that you put into this project.

My fellow members of the Aus-band made long days in the office always worth it. To Arianna Cerreta, I hope you continue to find joy in poop and DNA. To Bri Winkle, unfortunately I am unable to say what I would like here but I think you know. To Kaitlyn Strickfaden, I would not have gotten anywhere with coding without you. Thank you for always answering even my most simple of R questions.

Dedication

Most importantly, I would like to thank my family and friends back home in South Carolina. To my best friends, Alan and Marty, thank you for always being a phone call away. To my parents, Mike and Michelle, thank you for always pushing me to pursue my dreams (even if it is 36 hours away from home). To my brothers Caleb, Joah, Micah, and Malachi, our Fortnite and COD sessions helped me to destress more than you know.

The community and family I found here in Moscow were invaluable to my mental and emotional health. To Grace Little, I am so glad our friendship has endured these long years since our first internship out of undergrad. Who would have thought we would both end up here? Anne Yen, you are one of the brightest and most creative souls I have ever met. To my archnemesis Elise Stacy, I appreciate our banter and you keeping me humble. As always, thank you to my other two musketeers, Molly Garrett and Peter Rebholz, for the many great times at Walenta. Molly, you have constantly been my voice of reason and long-term thinker. From early morning gym sessions to emotional breakdowns, I do not know where I would be without you. To my first lab mate and roommate Peter, it has been a long journey to get here but I would not have wanted to start or end it with anyone else. Thanks for making life the last four years fun and always reminding me to be “chill.”

Table of Contents

List of Tables

List of Figures

Chapter 1: Estimating unmarked black bear populations using remote cameras

Introduction

Wildlife agencies are often tasked with managing game populations using limited resources or information. Many agencies rely on hunter reporting through various methods as their primary source for annual harvest estimates, ranging from mail-in surveys to check stations (Rupp et al. 2000, Beston and Mace 2012). While some states use mandatory or incentivized programs to increase hunter response, rarely is a 100% reporting rate achieved (Rupp et al. 2000). Lack of hunter response can lead to biased estimates of harvests (and therefore populations) and requires managers to account for imperfect reporting rates (Rosenberry et al. 2004). While estimating populations with imperfect reporting rates is possible, there are other drawbacks and it often requires additional information (Roseberry and Woolf 1991). Many models rely on data such as hunter effort that often varies year to year (Beston and Mace 2012). Population models that rely on harvest can be reliable tools for demonstrating trends in population abundance over time (Davis et al. 2007), however, they fail to show trends until several years of data have been analyzed, giving managers less time to react and alter significant changes in the population trend (Beston and Mace 2012). Additionally, most species have differing rates of harvest dependent upon size and sex that further limit the accuracy of harvest based abundance models due to unequal sample sizes (Tilton 2005).

Striving to understand population trends more precisely, some states have opted for other methods of estimating populations. Premiere among these has been mark-recapture models using noninvasive genetic data because it is useful on less abundant and cryptic species and provides a variety of information beyond simple abundance estimates (Stenglein et al. 2010, McCall et al. 2013). The widespread use of noninvasive genetic sampling has significantly decreased the number of personnel hours required for sampling and the need for invasive handling procedures (Mumma et al. 2015). Even with its relatively low costs compared to traditional capture and mark approaches, noninvasive genetic sampling can be difficult to scale to the levels in which most states usually manage species (Coster et al. 2011).

Mark-recapture methods have been expanded through the use of passive detectors (e.g. trail camera) when individual animals are uniquely marked or individually identifiable (Karanth 1995, Rowcliffe et al. 2008, Parsons et al. 2017). Identifying individuals through trail cameras has successfully been applied primarily with large cat species using features such as the stripe patterns of tigers (*Panthera tigris*; Karanth 1995) and the spot patterns of snow leopards (*Uncia uncia*; Jackson et al. 2006). However, most game species of management concern in the United States do not have these unique features. Animals must be physically captured and marked before being 'recaptured' with a trail camera (Chandler and Royle 2013).

New modeling approaches have found ways to estimate unmarked population abundance (Rowcliffe et al. 2008, Chandler and Royle 2013). These models, while useful, often require additional information or are only adequate for populations that occur at high densities (Loonam 2019). The random encounter model developed by Rowcliffe et al. (2008) circumvents many of these problems by using randomly placed cameras that estimate density as a function of trapping rate. Issues arise with the random encounter model when factoring in the tendency of trail cameras' infrared sensors to be highly variable at detecting species based on body size and the effect that habitat, temperature, and camera malfunctions have on detection rate (Rowcliffe et al. 2011, Burton et al. 2015).

The time-to-event and space-to-event models further the random encounter model and address the issue of variable detection rate (Moeller et al. 2018). The time-to-event model (TTE) follows similar assumptions as the REM, requiring independent estimates of movement rate and randomly placed cameras with measured viewsheds (Moeller et al. 2018). The TTE estimates density by measuring the amount of elapsed time until an animal is photographed (or captured). When a species persists at higher densities, there will be shorter time periods between photographs. Encounter histories for the TTE are determined by separating a photograph stream from a single camera into occasions and periods. A period is how long it would take an animal to cross a camera viewshed using a mean movement rate of the population. Occasions contain a set number of periods with a 'rest' time in between occasions. The period in which an animal is counted in the viewshed becomes the TTE. Occasions with no TTE are right censored.

The space-to-event model (STE) removes the variability of motion detection that can occur in the TTE using most trail camera's built in abilities to take photographs at specific intervals (Moeller et al. 2018). By using timelapse photographs and a measurable viewshed area, the need for movement rate and motion triggered photos is eliminated, removing variability that can occur in both. Animal density instead is determined by the amount of space surveyed (i.e., camera viewsheds) between detections. If less space is surveyed between detections, animals occur at higher densities. In the STE, the period length becomes the interval at which time-lapse photographs are taken (e.g., 10 minutes) with the occasion becoming the number of cameras that must be surveyed before coming across an animal. Both the TTE and STE models have shown promise and successfully been used to estimate elk (*Cervus canadensis*; Moeller et al.) and mountain lion (*Puma concolo*r; Loonam 2019) population sizes in Idaho.

Black bears (*Ursus americanus*) in Idaho have historically been managed using harvest data from mandatory hunter checks. Black bear harvest is not equal among all age and sex classes nor are all bears equally susceptible to capture methods, making both population reconstruction and mark-recapture modeling difficult (Diefenbach et al. 2004). Additionally, black bears are found in the majority of mountain forests throughout the state (Beecham and Rohlman 1994) making large scale capture projects not financially viable. Finding accurate and precise methods of estimating black populations in Idaho, while keeping costs low, is a critical goal of managers in the state. Black bears are an ideal study species to test the utility of the TTE and STE models. Their preference for forested habitat makes aerial and sight surveys difficult and leave trail cameras as one of the most effective methods of 'capture'. Randomly placed cameras that are not stratified to roads and trails are likely to observe black bears since they move randomly throughout the landscape and use roads and trails less frequently than other carnivores (Young and Beecham 1986, Kasworm and Manley 1990).

The objective of my study is to test the utility of the TTE and STE models as a new, noninvasive, and cost-effective method to estimate black bear populations in Idaho. We aim to test several methods of camera deployments and address all assumptions of the model so that these models can be applied to black bears in other states and additional species.

Methods

Study Areas

The study areas for my project were selected by the Idaho Department of Fish and Game (IDFG) across three different regions (Panhandle, Clearwater, and Southwest) and consisted of a Game Management Unit as the study area in each region: GMUs 6, 10A, and 32A, respectively (Fig. 1.1). The most northern of these units, GMU 6 (hereafter St. Joe study area), is 2,726 km^2 and located in Region 1, the Panhandle Region. Around 40% of the unit is managed by the U.S. Forest Service (USFS) within the St. Joe National Forest and is a frequented location for summer recreation. The remaining land contains 40% privately owned land (largely by the logging company PotlatchDeltic), 10% state of Idaho, and 10% split between BLM and Bureau of Indian Affairs.

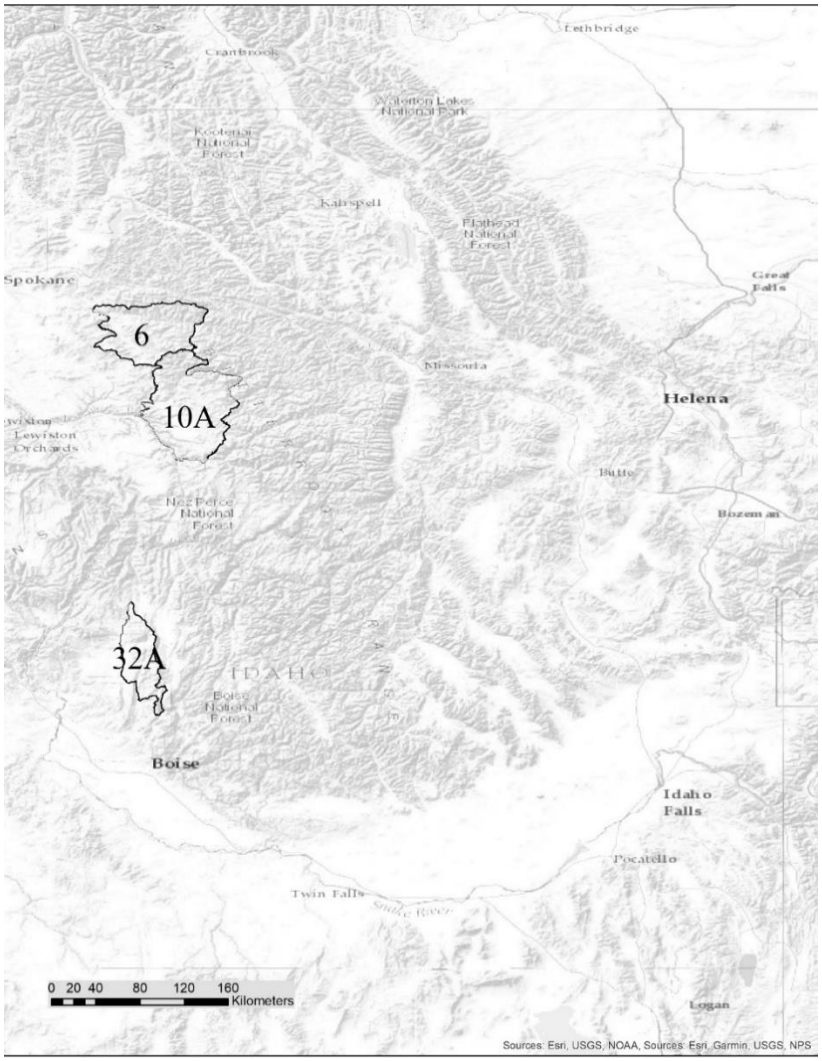

Figure 1.1: A satellite map of Idaho, USA with the outlines of three IDFG Game Management Units used as study areas to estimate black bear density from cameras: St. Joe (GMU 6), Clearwater (GMU 10A), and Council (GMU 32A).

Black bears in the St. Joe study area are managed through general harvest spring (Apr. 15 – June 30) and fall (Aug 30. – Nov. 30) hunting seasons. Dog training is allowed July 1 – July 31 and dogs allowed during all open seasons except for Aug. 30 – Sep. 14 and Oct. 10 – Oct. 31. Hunters may also purchase a second bear tag for use during the season and baiting is allowed. During the 2018 season prior to the start of this project 117 bears were harvested from the unit with 90 of those during the spring season.

The largest of the three study areas, GMU 10A (hereafter Clearwater study area), is

4,028 km^2 and is in the Clearwater Region (R2). Approximately 50% of the unit consists of private land, 24% USFS managed land within the Nez Perce-Clearwater National Forest, and 24% State of Idaho Managed Land. Black bears in the Clearwater study area are also managed through a general harvest spring (Apr. 15 – May 31) and fall (Aug. 30 – Oct. 31) hunting season with dog training allowed June 1 – July 31. Dogs are prohibited Apr. 15 – 30, Aug. 30 – Sep. 14, and Oct. 10 – Oct. 31. Baiting was prohibited until the fall 2019 season. In 2018, 110 bears were harvested split evenly between both fall and spring seasons.

The southernmost unit is GMU 32A (hereafter Council study area) located in the Southwest Region (R3) and is the smallest study area at 1,545 km^2. The Council study area is majority public land (70%) with the eastern two-thirds in the Payette National Forest and the southern areas within the Boise National Forest. The remaining public land is a mixture of BLM (9%) and State of Idaho (3%) intermixed with private. The entire unit is used for cattle grazing throughout the summer months as part of grazing permits and allotments. Black bears in the Council study area are managed through controlled hunts. The spring (Apr. 1 – May 22) hunting season has a draw of 40 tags and the fall (Aug. 15 – Aug. 31) hunting season a draw of 100 tags on private land only and Sep. 1 – Oct. 31 for the whole unit (these tags can be used in this unit and an adjacent GMU). The 2018 season had a total harvest of 2 bears with both bears harvested during the fall season.

Field Methods

Captures & Movement Rates

The TTE model requires an independent estimate of movement rate. To obtain independent estimates of movement rate, we captured and collared black bears in each of the three study areas. Bears were captured using Aldrich spring-activated foot snares set in ‘cubbies’ at the base of trees. We set traplines in summer 2019 for the St. Joe and Council study areas, all three study areas in summer 2020, and only the St. Joe study area in 2021.

We darted captured bears using a Pneu-Dart (Pneu-Dart, Inc., Williamsport, PA) pressurized rifle and immobilized them with 2cc darts at 1.1 mg/45 kg of a Telazol® (286 mg Tiletamine, 286 mg Zolazepam)/Xylazine mixture (3.3 ml of 100 mg of Xylazine to 1 bottle

of 572 mg Telazol®) and water. Tolazoline (200 mg/ml) was used for the reversal of Xylazine. All our captures were conducted under the University of Idaho Institutional Animal Care and Use Committee protocol (IACUC 2019-05 – *Developing Methods for Black Bear Population Monitoring*).

Bears of various sex and age classes greater than 34kg were given a Telonics TGW-4570-4 GPS/Iridium collar. Initially, we collected bear location frequencies every four hours during peak activity months (May – September). Low numbers of captures in 2019 provided extra battery life for the remainder of the study and allowed us to increase location frequencies to 24 locations/day from May 1 – October 1 in 2020 and 2021. The GPS collars had automatic drop offs set to detonate August 1, 2021. We obtained hourly movement rates using only location points during the camera deployment period to coincide with seasonal changes in black bear movement.

Camera Deployment

In 2019, we attempted to strictly uphold the requirements and assumptions of the TTE and STE models; primarily that cameras be placed randomly without regards to roads or trails (Moeller et al. 2018). Black bears use roads and trails less frequently than other carnivores like mountain lions or wolves (*Canis lupus*) which frequent remote roads, trails, and game trails (Beecham and Rohlman 1994, Loonam 2019, Ausband et al. 2022). As such, we assumed that completely random cameras would have obtain sufficient detections of black bears to run the TTE and STE models.

We overlaid each study area (ArcGIS 2020) with a grid containing squares of 25km^2 in 2019. Grids containing more than 50% of the grid inside the unit boundary received a true random primary location. The actual camera location could be within 200 meters of the random location to ensure the clearest viewshed. The camera was placed approximately 1.5 – 2 meters high on a tree 15 meters south of the random point and pointed north. We established and marked with flagging the viewshed area at 30m distance from the center of the camera. The viewshed width was established by placing flagging at 3.5m distances from the 30m center point to a maximum of 10.5 meters. We cleared as much dense vegetation as

possible to ensure clear viewsheds and measured the farthest viewable distance for each cone. The cameras were set at high sensitivity to take a group of three photos upon motion detection. Additionally, cameras were set to take a timelapse photograph every 10 minutes (e.g., 13:10:00, 13:20:00)

We cooperated with IDFG to increase the number of deployed cameras in 2020 and 2021. IDFG personnel deployed cameras in the St. Joe and Clearwater study areas; ungulate style cameras (or cameras deployed with complete randomness; hereafter "random cameras") and paired predator style cameras (cameras targeted to the closest road or trail to the random point to increase predator detections; hereafter "targeted cameras"). In the Council study area, we deployed only targeted cameras. The change in deployment allowed for comparison between random deployment and targeted deployment styles for each of the models.

TTE Model

The TTE model assumes that animals are Poisson-distributed across the landscape and the time until an encounter event occurs is exponentially distributed around density (Eq. 1, Moeller et al. 2018). For example,

$$\mathrm{TTE} \sim \mathrm{Exp}(\lambda) \qquad \text{(Equation 1)}$$

imagine we are looking for a bear on a mountain side with a spotting scope. The spotting scope is stationary on a set location while we wait for a bear to come into view. Assuming that bears are Poisson distributed, the amount of time it takes to spot a bear is indicative of the density of bears on the mountainside.

The TTE follows these assumptions using randomly placed trail cameras set to take motion trigger photos. Separating each camera $i = 1, 2, \ldots, M$, into sampling occasions $j = 1, 2, \ldots, J$, and sampling periods $k = 1, 2, \ldots, K$ we can begin to create an encounter history. The sampling period requires independent estimates of movement rate and is a function of the bear's movement rate divided by the square root of the viewshed area, or the time it would take a bear to cross the viewshed. When accounting for right-censored data (no detections) the result is Eq. 2 (Moeller et al. 2018) representing the exponential likelihood

and giving $\hat{\lambda}$, or the number of animals present in a

$$\mathcal{L}\left(\lambda|T_{ij}\right) = \prod_{j=1}^{J} \prod_{i=1}^{M} \begin{pmatrix} {}^{I_{(T_{ij} \leq K)}} \lambda e^{T_{ij}} \\ +\left(1-I_{(T_{ij} \leq K)}\right) e^{-\lambda T_{ij}} \end{pmatrix} \qquad \text{(Equation 2)}$$

camera's viewshed. The density of bears can be derived by dividing $\hat{\lambda}$ by the mean area of all the camera's viewsheds $\bar{a}$. Total abundance can then be found by multiplying density by the size of the study area.

Our analysis of the TTE model included a "single run" (or non-bootstrapped estimate) of all models for both the random and targeted style deployments. We populated the TTE using two sets of data for comparisons, 1) motion triggered photos only, and 2) motion triggered photos and timelapse photos (or "all photos"). We generated population estimates in Program R (R Core Team 2021) using the spaceNtime package (Moeller et al. 2018).

There was an increase in motion triggered photographs from cameras in 2021. Additionally, there were often "outlier" cameras present, or cameras that contained a high percentage of all motion triggered photographs. To reduce this potential bias, we bootstrapped the TTE models 1,000 times by sampling with replacement. This bootstrapping method was applied to all TTE model iterations.

STE Model

The STE functions similarly to the TTE but removes variability from motion detections by collapsing each sampling occasion to a single instance in time. Returning to our example with the spotting scope, instead of leaving the scope on one location as in the TTE model, we move the spotting scope around the mountainside at set intervals hoping to locate a bear. In this scenario (under the same assumption of Poisson distribution), we are measuring the amount of space between bears to determine density.

The STE model uses the same breakdown of encounter histories S_j where j = 1, 2, …, J, and sampling occasions i = 1, 2, …, M (where M equals number of cameras). The equation is the TTE model with the movement rate dimension removed (Eq. 3, Moeller et al. 2018).

$$\mathcal{L}(\lambda|S_j) = \prod_{j=1}^{J} \left(I_{(S_j \leq K)} \lambda e^{S_j} + \left(1 - I_{(S_j \leq M)}\right) e^{-\lambda S_j} \right) \quad \text{(Equation 3)}$$

Since the model relies on accurate measurements of camera viewshed area for each camera, we did not use an average area as in the TTE, but measured each camera's viewshed individually. Abundance is found by multiplying density by the size of the study area. We generated population estimates in Program R (R Core Team 2021) using the spaceNtime package (Moeller et al. 2018).

We populated the STE using two sets of data for comparisons, 1) timelapse photos only, and 2) timelapse photos and motion triggered photos. The sampling length of the STE model (10 seconds) allows for motion photos that occurred close to the timelapse interval of 10 minutes to be included in the model. There are frequently few timelapse photographs despite extensive camera deployments. Including an additional 10 seconds on either side of the interval allows for the inclusion of photos that were not quite on the exact 10 minute mark but is not an extensive interval to where it would violate assumptions.

Bootstrapping

There was an increase in motion triggered photographs from cameras in 2021. Additionally, there were often "outlier" cameras present, or cameras that contained a high percentage of all motion triggered photographs. To reduce this potential bias, we bootstrapped the TTE models 1,000 times by sampling with replacement. This bootstrapping method was applied to all TTE model iterations. We also bootstrapped the STE across all model iterations as a means of comparison for the TTE.

Density Comparisons

We compared abundance and density estimates of historic black bear populations in the three study areas and those of populations found in similar habitats in the montane west (Beecham and Rohlman 1994, Stetz et al. 2014, Loosen et al. 2019, Welfelt et al. 2019). Loosen et al. (2019) estimated black bear densities in Alberta across different land use types

using spatially explicit capture-recapture (SECR) and resource-selection functions (RSF). We only used those results from SECR estimates and combined their estimates of male and female black bears. Black bear densities differed dependent upon land use types with a mean of 12.6 bears/100 km^2 on private land, 5.44 bears/100 km^2 on public, and 33.13 bears/100 km^2 in protected areas (Loosen et al. 2019). We simplified this to a mean density of 12.6 bears/100 km^2.

Stetz et al. (2014) estimated black bear densities in Glacier National Park using non-invasive genetic sampling from hair traps and bear rubs and increased the precision of their estimates using a correction for sampling effort in the form of a full and one-half mean maximum distance moved. Their results found a density estimate of 11.4 bears/100 km^2 (Stetz et al. 2014). Welfelt et al. (2019) estimated black bear densities in the North Cascades with their study area separated into two areas: western north Cascades and eastern North Cascades. Their research was a four year project that used non-invasive DNA collection and physical captures of black bears. Bear densities in the eastern North Cascades, with habitat comparable to the Council study area, had black bear densities ranging from 7.1 bears/100 km^2 to 33.6 bears/100 km^2 (Welfelt et al. 2019). We used the mean of this range with 20.1 bears/100 km^2. The western North Cascades, with habitat comparable to the St. Joe and Clearwater study areas, had black bear densities ranging from 13.5 bears/100 km^2 to 27.8 bears/100 km^2 with a mean of 20.1 bears/100 km^2 (Welfelt et al. 2019).

The most comparable studies were conducted by Beecham and Rohlman (1994) in six different locations in Idaho with capture efforts conducted in two of our study areas, the Council and St. Joe study areas. Using capture-mark-recapture and population reconstruction methods they found bear density estimates of 38.61 bears/100 km^2 in areas analogous to the St. Joe and Clearwater study areas. Bear densities within the Council study area were estimated at 57.9 bears/100 km^2. Overall, the comparable density ranges from the literature were 11.4 – 38.61 bears/100 km^2 in the St. Joe and Clearwater study areas while Council ranged from 11.4 – 57.9 bears/100 km^2. Black bears in the Council study area are managed through a controlled hunt and historic estimates were much higher in that unit, account for the higher upper end of the comparable density ranges.

Results

Camera Deployment

In 2019, we deployed 195 randomly placed cameras across the three units (84, 67, and 44 cameras in the St. Joe, Clearwater, and Council study areas, respectively). In 2020 and 2021, we deployed 150 randomly placed cameras in both the St. Joe and Clearwater study areas. These study areas used 100 of the 150 random points to place a paired targeted on the nearest road or trail. The Council study area had only 75 targeted cameras but followed the same process as the other units by creating random points first, then placing a camera location on the closest road or trail to that point.

Across all cameras from 2019 there were only 9 timelapse photographs of bears, leading to the change in camera deployment size and style in 2020 and 2021 as we attempted to increase probability of detection. The results was an increase in both timelapse and motion photos for both years (Table 1.1).

Table 1.1: Number of cameras deployed and total number of timelapse and motion photos for each deployment type (i.e., random and targeted) in three study areas in Idaho, USA, 2019 – 2021.

Study Area	Number of Cameras		Timelapse Photos		Motion Photos	
	Random	Targeted	Random	Targeted	Random	Targeted
2019						
St. Joe	84	-	1	-	61	-
Clearwater	67	-	4	-	52	-
Council	44	-	4	-	15	-
2020						
St. Joe	150	100	12	9	484	949
Clearwater	150	100	6	2	480	808
Council	-	61	-	19	-	1,579
2021						

St. Joe	150	100	30	9	2,086	949
Clearwater	150	100	12	4	1,397	933
Council	-	75	-	8	-	2,347

Movement Rates

Over the course of our three field seasons, we had a total of 49 captures (Table 1.2). We divided hourly movement rates by 3,600 seconds to obtain the time in meters/second needed for the TTE model. The hourly movement rates in 2020 ranged from 227 – 279 m/hr. and ranged from 210 – 224 m/hr. in 2021 (Table 1.3). We did not pool movement data across study areas or years due to variability in bear movement rates between years and each study area consisting of different habitat types with varying harvest pressure. Additionally, mean movement rate was skewed high from larger movement rates of adult males and juvenile bears, therefore we used a median movement rate for each study area and year.

Table 1.2: Number of black bears captured and radiocollared (Global Positioning System) in three study areas in Idaho, USA, 2019 – 2021. Resulting location data were used to estimate movement rates and populate a time to event model for density estimation.

Study Areas	2019	2020	2021
St. Joe	1	12	2
Clearwater	0	17	0
Council	4	13	0
Total	5	42	2

Table 1.3: Median movement rates of black bears in meters/hour and meters/second for three study areas in Idaho, USA, 2019 – 2021. Movement rates were used to populate a time to event model and estimate bear density.

Study Area	2019		2020			2021		
	m/hr	m/sec	m/hr	m/sec	N (Number of Bears)	m/hr	m/sec	N (Number of Bears)
St. Joe	-	-	279.16	0.078	8	224.13	0.0623	8
Clearwater	-	-	264.36	0.073	12	209.96	0.0583	7
Council	169.19	0.047	227.03	0.063	11	209.96	0.0583	7

Time to Event (TTE)

Abundance and density estimates were similar when using just motion photos or motion and timelapse photos (Table 1.4). In 2020, the St. Joe study area had TTE abundance estimates of 776 (586 – 1,027, 95% CI) bears and a density of 28 bears/100 km^2 (21 – 38, 95% CI) from random camera deployment and 6,858 (5,141 – 9,148, 95% CI) bears and a density of 251 (189 – 335, 95% CI) from targeted camera deployment (Fig. 1.2). The Clearwater study area had abundance estimates of 738 (114 – 545, 95% CI) bears and 1,787 (1,302 – 2,453, 95% CI) bears from random and targeted camera deployments, respectively, with density estimates of 18 bears/100 km^2 (14 – 25, 95% CI) and 44 bears/100 km^2 (32 – 61, 95% CI; Fig. 1.3). The Council study area had an abundance estimate of 908 (759 – 1,086, 95% CI) bears and a density estimate of 59 bears/100 km^2 (49 – 70, 95% CI) from the targeted deployment (Fig. 1.4). These estimates represent models ran including all data sources since there tended to be minimal difference between using a single data source or both. Results from all model iterations are represented in Table 1.4.

Table 1.4: Black bear (*Ursus americanus*) population estimates using cameras and a time-to-event model for three study areas, two camera deployment styles, and multiple data sources in Idaho, USA, 2020 – 2021. M = motion-trigger photos, T = timelapse photos. Comparable density ranges derived from Beecham and Rohlman 1994, McCall et al. 2013, Stetz et al. 2014, Loosen et al. 2019, Welfelt et al. 2019.

Study Area	Deployment Type	Data Source (Photo Type)	N	95% CI	Density (bears/100 km^2)	% Within Comparable Range	N	95% CI	Density (bears/100 km^2)	% Within Comparable Range
					2020				2021	
St. Joe	Random	M	759	571 – 1,008	21 – 37	100%	1,044	837 – 1,302	31 – 48	47%
St. Joe	Random	M & T	776	586 – 1,027	21 – 38	100%	1,118	903 – 1,384	33 – 51	33%
St. Joe	Targeted	M	6,770	5,066 – 9,047	186 – 332	0%	721	549 – 945	21 – 35	100%
St. Joe	Targeted	M & T	6,858	5,141 – 9,148	189 – 335	0%	733	561 – 959	21 – 35	100%
Clearwater	Random	M	728	537 - 987	13 - 24	100%	2,277	1,869 – 2,776	46 – 69	0%
Clearwater	Random	M & T	738	545 – 998	14 – 25	100%	2,321	1,908 – 2,824	47 – 70	0%
Clearwater	Targeted	M	1,743	1,265 – 2,402	31 – 60	28%	5,661	4,475 –	111 – 178	0%

								7,160		
Clearwater	Targeted	M & T	1,787	1,302 – 2,453	32 – 61	24%	5,661	4,475 – 7,160	111 – 178	0%
Council	Targeted	M	891	744 – 1,067	48 – 69	48%	4,226	3,650 – 4,893	236 – 317	0%
Council	Targeted	M & T	908	759 – 1,086	49 – 70	43%	4,227	3,651 – 4,895	236 – 317	0%

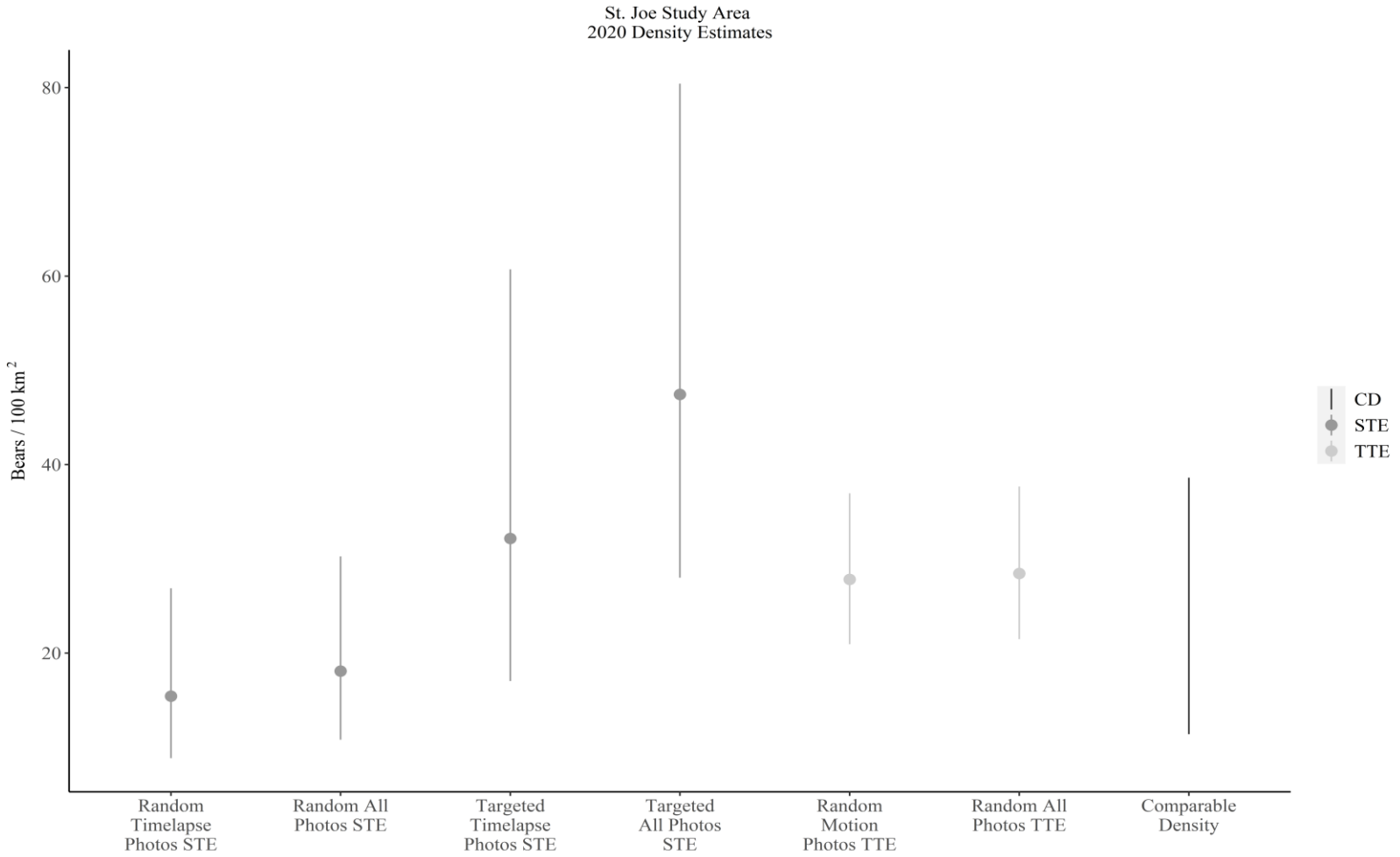

Figure 1.2: Black bear (*Ursus americanus*) population estimates in 2020 using cameras and a time-to-event and space-to-event model for two deployment styles and multiple data sources in the St. Joe study area (2,727 km^2), Idaho, USA, 2020. Comparable density (CD) estimates are derived from Beecham and Rohlman 1994, Stetz et al. 2014, Loosen et al. 2019, Welfelt et al. 2019. Results far outside of comparable density were removed from figures to make scales more viewable.

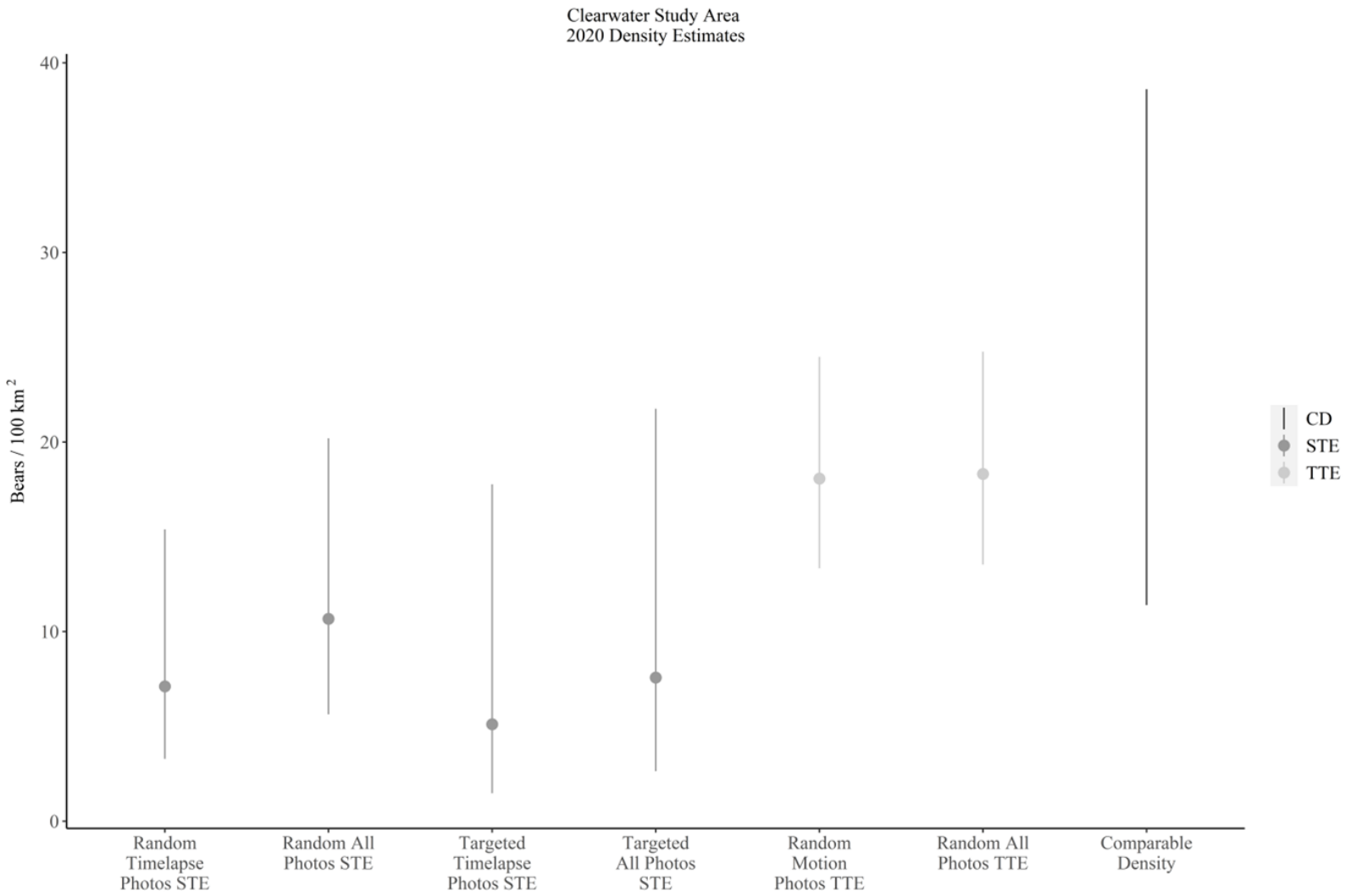

Figure 1.3: Black bear (*Ursus americanus*) population estimates in 2020 using cameras and a time-to-event and space-to-event model for two deployment styles and multiple data sources in the Clearwater study area (4,029 km^2), Idaho, USA, 2020. Comparable density (CD) estimates are derived from Beecham and Rohlman 1994, Stetz et al. 2014, Loosen et al. 2019, Welfelt et al. 2019. Results far outside of comparable density were removed from figures to make scales more viewable.

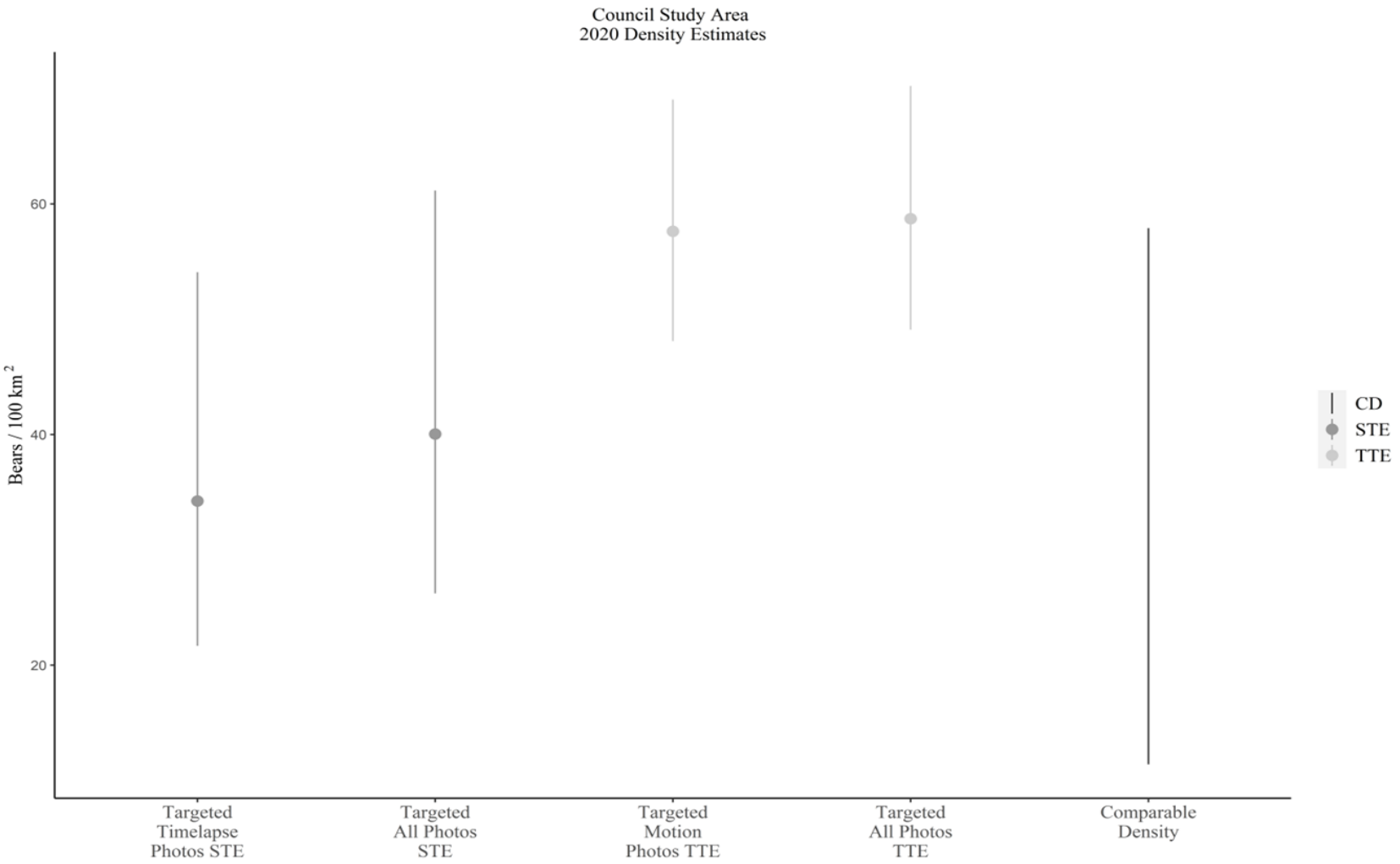

Figure 1.4: Black bear (*Ursus americanus*) population estimates in 2020 using cameras and a time-to-event and space-to-event model for two deployment styles and multiple data sources in the Council study area (1,546 km^2), Idaho, USA, 2020. Comparable density (CD) estimates are derived from Beecham and Rohlman 1994, Stetz et al. 2014, Loosen et al. 2019, Welfelt et al. 2019. Results far outside of comparable density were removed from figures to make scales more viewable.

TTE single run (i.e., non-bootstrapped) estimates for 2021 varied considerably using random and targeted camera deployments. Both motion photos and motion and timelapse photo estimates were again similar (Table 1.5). St. Joe study area abundance estimates were 1,118 (903 – 1,1384, 95% CI) bears with density estimates of 44 bears/100 km^2 (33 – 51) and abundance estimates of 733 (561 – 959, 95% CI) bears and density estimates of 27 bears/100 km^2 (21 – 35, 95% CI) for random and targeted deployment, respectively (Fig. 1.6). Clearwater study area abundance estimates for random deployment were 2,321 (1,908 – 2,824, 95% CI) bears and density estimates of 58 bears/100 km^2 (47 – 70, 95% CI). Targeted deployment abundance estimates were 5,661 (4,475 – 7,160, 95% CI) with density estimates of 140 bears/100 km^2 (111 – 178, 95% CI; Fig. 1.3). Abundance estimates were 4,227 (3,651 – 4,895, 95% CI) bears and density estimates of 273 bears/100 km^2 (236 – 317, 95% CI) in the Council study area (Fig. 1.7). Population estimates from TTE models in 2020 and 2021 were higher than comparable density from the literature in 14 of 20 (70%) of comparisons (Table 1.4).

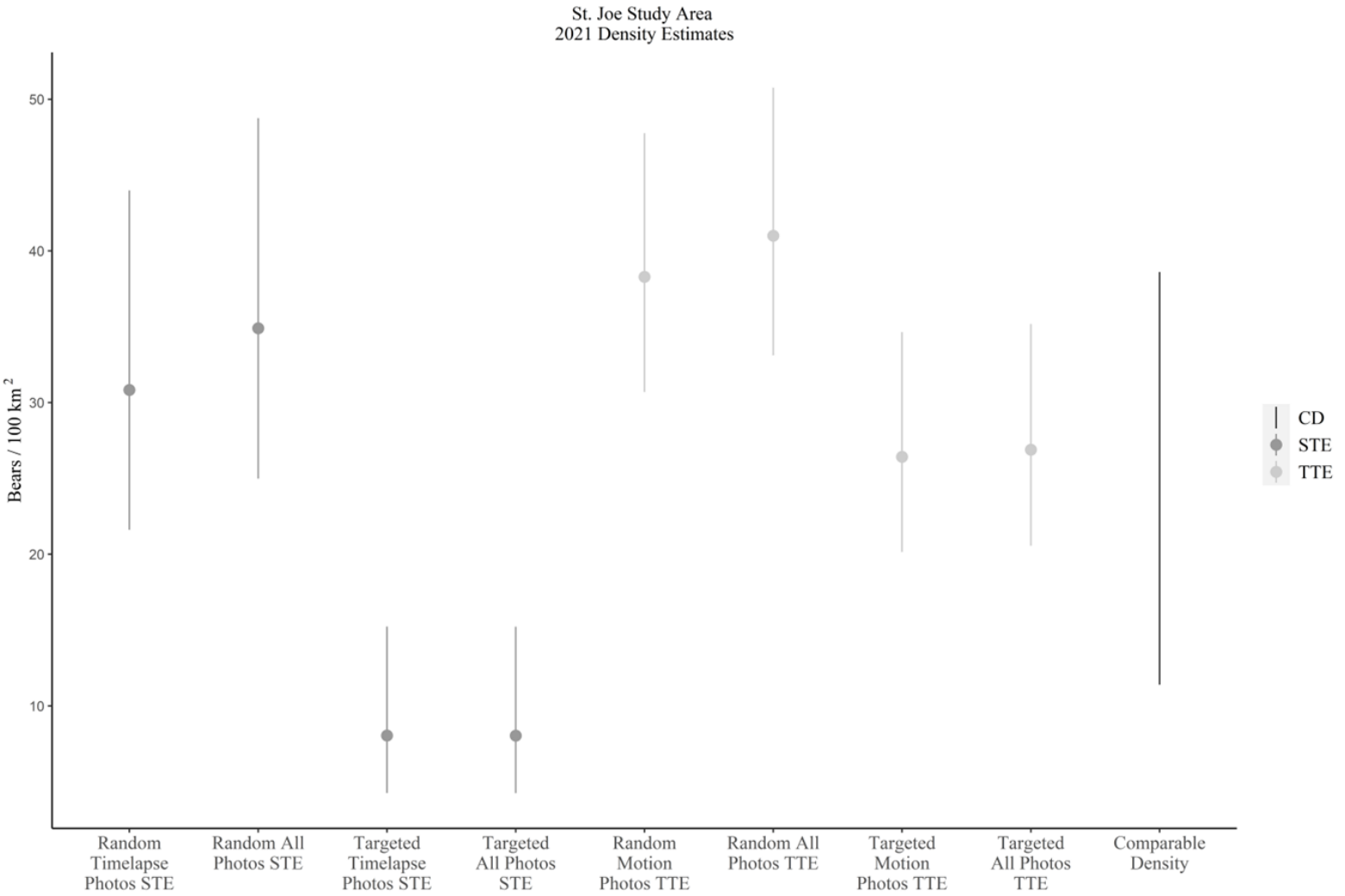

Figure 1.5: Black bear (*Ursus americanus*) population estimates in 2021 using cameras and a time-to-event and space-to-event model for two deployment styles and multiple data sources in the St. Joe study area (2,727 km^2), Idaho, USA, 2021. Comparable density (CD) estimates are derived from Beecham and Rohlman 1994, Stetz et al. 2014, Loosen et al. 2019, Welfelt et al. 2019. Results far outside of comparable density were removed from figures to make scales more viewable.

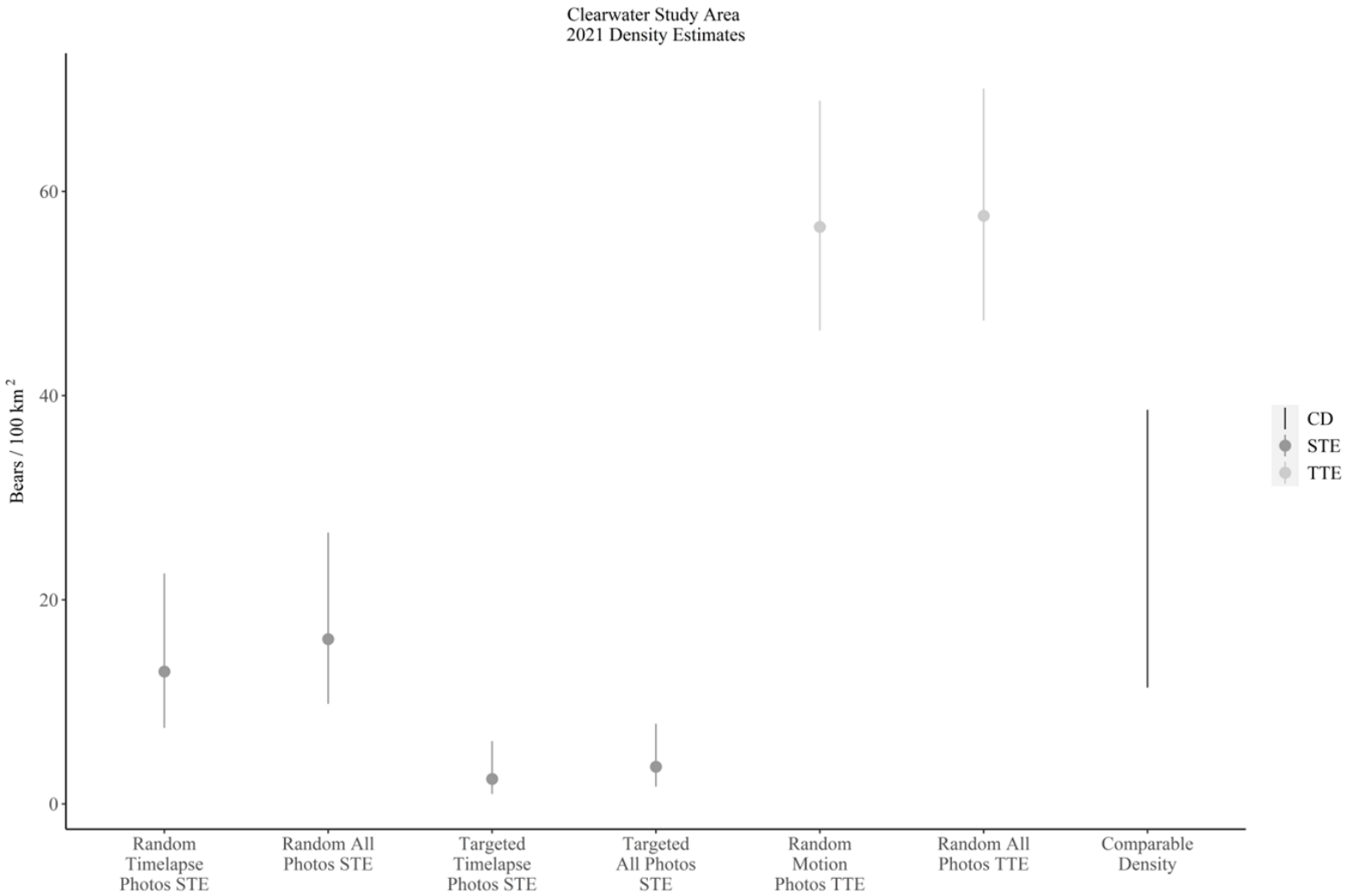

Figure 1.6: Black bear (*Ursus americanus*) population estimates in 2021 using cameras and a time-to-event and space-to-event model for two deployment styles and multiple data sources in the Clearwater study area (4,029 km^2), Idaho, USA, 2021. Comparable density (CD) estimates are derived from Beecham and Rohlman 1994, Stetz et al. 2014, Loosen et al. 2019, Welfelt et al. 2019. Results far outside of comparable density were removed from figures to make scales more viewable.

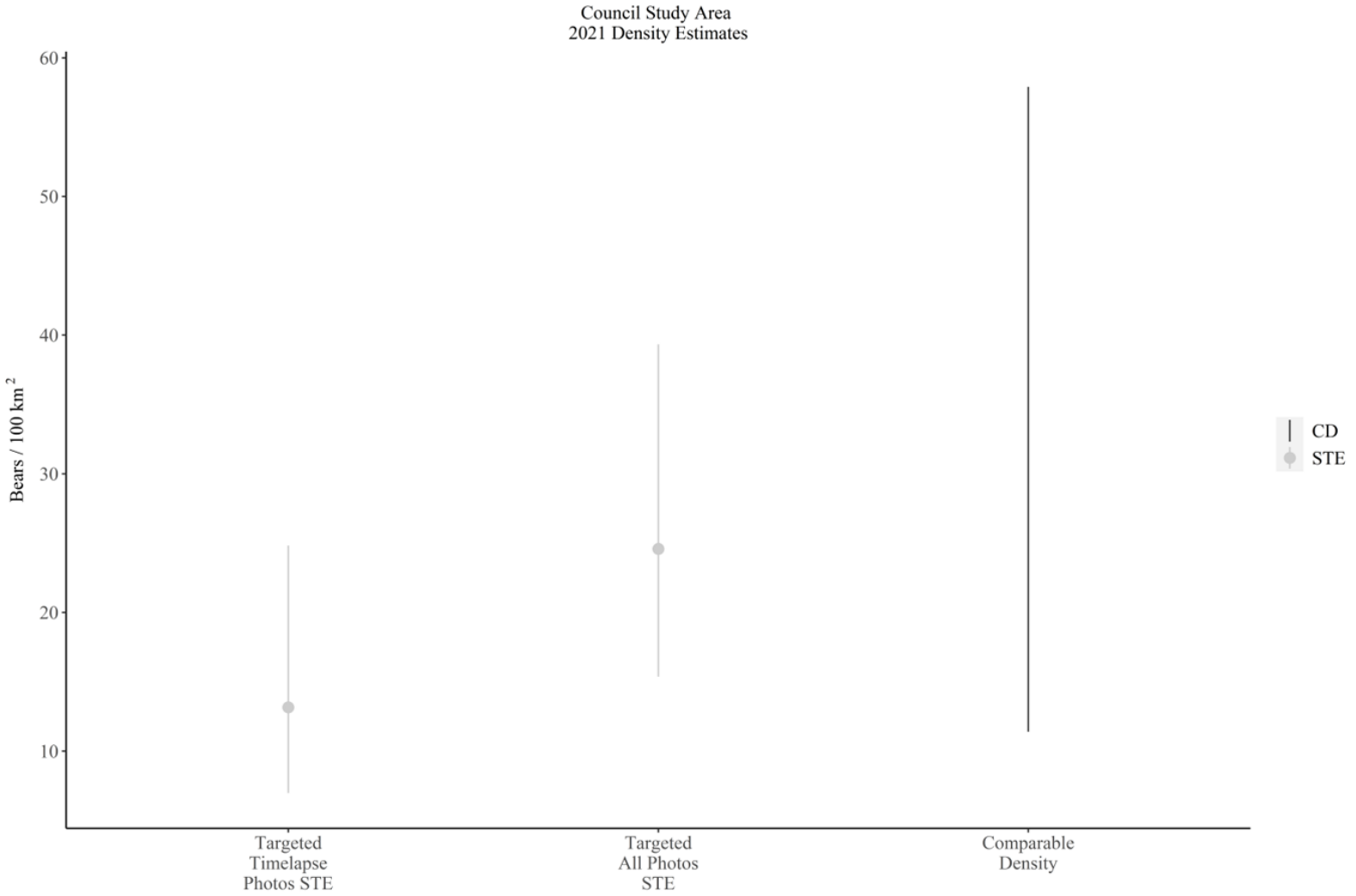

Figure 1.7: Black bear (*Ursus americanus*) population estimates in 2021 using cameras and a time-to-event and space-to-event model for two deployment styles and multiple data sources in the Council study area (1,546 km^2), Idaho, USA, 2021. Comparable density (CD) estimates are derived from Beecham and Rohlman 1994, Stetz et al. 2014, Loosen et al. 2019, Welfelt et al. 2019. Results far outside of comparable density were removed from figures to make scales more viewable.

Space to Event (STE)

Model iterations from STE estimates were also similar between timelapse only photo estimates and timelapse and motion photo estimates in 2020. Including the few motion trigger photos that occur within the 10 second bounding interval for cameras with low timelapse photo slightly increased STE estimates. In 2020, the St. Joe study area had abundance estimates of 493 (295 – 825, 95% CI) bears and density estimates of 18 bears/100 km^2 (11 – 30, 95% CI) from random deployment and abundance estimates of 1,294 (764 – 2,193, 95% CI) bears and density estimates of 47 bears/100 km^2 (28 – 80, 95% CI) from targeted deployment (Fig. 1.2). The Clearwater study area had abundance estimates of 430 (227 – 814, 95% CI) bears from random deployment and 305 bears (106 – 876, 95% CI) bears from targeted deployment. Density estimates were 11 bears/100 km^2 (6 – 20, 95% CI) and 8 bears/100 km^2 (3 – 22, 95% CI), respectively (Fig 1.3). Abundance estimates from targeted deployment in Council were 619 (405 – 945, 95% CI) bears with a density estimate of 40 bears/100 km^2 (26 – 61, 95% CI; Fig. 1.4)

Table 1.5: Black bear (*Ursus americanus*) population estimates using cameras and a space-to-event model for three study areas, two deployment styles, and multiple data sources in Idaho, USA, 2020 – 2021. M = motion-trigger photos, T = timelapse photos. Comparable density ranges derived from Beecham and Rohlman 1994, Stetz et al. 2014, Loosen et al. 2019, Welfelt et al. 2019.

Study Area	Deployment Type	Data Source (Photo Type)	N	95% CI	Density (bears/100 km^2)	% Within Comparable Range	N	95% CI	Density (bears/100 km^2)	% Within Comparable Range
					2020				2021	
St. Joe	Random	M	421	241 – 733	9 – 27	89%	841	589 – 1199	22 – 44	77%
St. Joe	Random	M & T	493	295 – 825	11 – 30	100%	952	681 – 1330	25 – 49	58%
St. Joe	Targeted	M	877	465 – 1,656	17 – 61	50%	220	116 – 415	4 – 15	55%
St. Joe	Targeted	M & T	1,294	764 – 2,193	28 – 80	21%	219	116 – 415	4 – 15	55%
Clearwater	Random	M	287	132 – 620	3 – 15	33%	523	300 - 910	7 – 23	75%
Clearwater	Random	M & T	430	144 – 227	6 – 20	64%	651	395 – 1,071	10 – 27	94%
Clearwater	Targeted	M	206	59 – 716	1 – 18	41%	99	39 – 248	1 – 6	0%

Clearwater	Targeted	M & T	305	106 – 876	3 – 22	58%	147	68 – 317	2 – 8	0%
Council	Targeted	M	529	335 – 836	22 – 54	100%	204	108 – 384	7 – 25	78%
Council	Targeted	M & T	619	405 – 945	22 – 61	91%	380	238 – 608	15 - 39	100%

Similar to TTE, STE single run estimates for 2021 varied considerably using both random and targeted camera deployment types. Models ran using either timelapse only or timelapse and motion photos remained similar as in 2020. In the St. Joe study area for 2021, abundance and density estimates for random deployment were 952 (681 – 1,330, 95% CI) bears and 35 bears/100 km^2 (25 – 49, 95% CI), respectively. Targeted deployment abundance estimates were 219 (116 – 415, 95% CI) bears and density estimates were 8 bears/100 km^2 (4 – 15, 95% CI; Fig. 1.5). The Clearwater study area abundance estimates were 651 bears (395 – 1,071, 95% CI) and density estimates were 16 bears/100 km^2 (10 – 27, 95% CI) from random deployment. Clearwater study area targeted deployment abundance estimates were 147 (68 – 317, 95% CI) bears with a density estimate of 4 bears/100 km^2 (2 – 8, 95% CI; Fig. 1.6). Abundance estimates in the Council study area were 380 (238 – 608, 95% CI) bears with a density of 25 bears/100 km^2 (15 – 39, 95% CI; Figure 1.7). Estimates from the STE models had 95% CI's with at least 80% overlap with the range of comparable density from the literature in just 6 of 20 (30`%) comparisons (Table 1.5).

Time to Event Bootstrapping

Bootstrapping the TTE model across all camera deployment styles generally resulted in decreased estimates when single run estimates were high, although estimates from targeted camera deployments remained higher (approx. 120 – 350%) than density from comparable studies. Like the single run estimates of the TTE model, estimates did not vary considerably between analysis with only motion trigger and motion and timelapse photos. After bootstrapping over 1,000 iterations, the St. Joe Study area had a 3.5% lower bootstrapped abundance estimate in 2020 of 803 (SD = 320) bears and a mean density estimate of 29 bears/100 km^2 from random deployment and a 66% lower bootstrapped abundance estimate of 2,301 (SD = 1,537) bears and a mean density estimate of 84 bears/100 km^2 from targeted deployment. The Clearwater study area a 6% higher bootstrapped abundance estimates of 781 (SD = 132) bears from random deployment and an 8% higher targeted deployment estimate of 1,935 (SD = 983) bears with mean densities of 19 bears/100 km^2 and 48 bears/100 km^2, respectively. Council study area targeted deployment estimates increased by

128% with bootstrapping to an abundance estimate of 2,076 (SD = 1292) bears and a mean density estimate of 134 bears/100 km^2 (Table 1.6; Appendix A).

Table 1.6: Black bear (*Ursus americanus*) population estimates using cameras and a time-to-event model bootstrapped 1,000 times by sampling from cameras with replacement. Density estimates represent combined data sources of motion-trigger photos and timelapse photos. Comparable density estimate ranges derived from Beecham and Rohlman 1994, Stetz et al. 2014, Loosen et al. 2019, Welfelt et al. 2019.

Study Area	Deployment Type	N	SD	Density (bears/100 km^2)	% Within Comparable Range	N	SD	Density (bears/100 km^2)	% Within Comparable Range
				2020				2021	
St. Joe	Random	803	320	29 – 30	100%	1,204	188	44 – 45	0%
St. Joe	Targeted	2,301	1,537	81 – 88	0%	910	796	32 – 35	100%
Clearwater	Random	781	132	19 – 20	100%	1,884	285	46 – 47	0%
Clearwater	Targeted	1,935	983	47 – 50	0%	1,852	1,043	44 – 48	0%
Council	Targeted	2,076	1,292	129 – 139	0%	3,162	1,793	197 – 212	0%

Bootstrapping the TTE in 2021 followed the same general trend as 2020. The St. Joe TTE abundance estimate in 2020 with random deployment was 8% higher after bootstrapping and was 1,204 (SD = 188) bears and a mean density estimate of 44 bears/100 km^2. Targeted deployment estimates were 24% higher post bootstrapping and were 910 (SD = 796) bears and 33 bears/100 km^2 for abundance and density, respectively. Clearwater study area abundance estimates from random deployment were approximately 20% lower at 1,884 (SD = 285) bears with a mean density of 47 bears/100km^2 and targeted deployment abundance estimates were 67% lower at 1,852 (SD = 1,043) bears and mean density estimates of 46 bears/100 km^2. Council had a 25% lower abundance estimate after bootstrapping of 3,162 (SD = 1,793) bears and mean density estimate of 205 bears/100 km^2 (Table 6). Bootstrapped estimates of the TTE model produced 3 out of 10 (30%) density estimates that fell within the comparable density estimates from the literature (Table 6).

Space to Event Bootstrapping

STE model population estimates generally decreased after bootstrapping to less than estimates of a single iteration of the STE model and lower than comparable studies. The STE bootstrapping abundance estimates again followed the pattern of timelapse or motion and timelapse photos not making a considerable difference in the estimate. The St. Joe study area estimates in 2020 decreased 56% to an abundance estimate of 218 (SD = 53) bears and a mean density estimate of 8 bears/100 km^2 from random deployment. Targeted deployment estimates decreased 41% to an abundance estimate of 768 (SD = 176) bears and mean density estimates of 29 bears/100 km^2. The Clearwater study area abundance estimates were 10% lower with 388 (SD = 136) bears and mean density estimates of 10 bears/100 km^2 and 40% lower with 183 (SD = 79) bears and a density estimate of 5 bears/100 km^2 from random and targeted deployments, respectively. The Council study area abundance estimates also decreased 43% to 351 (SD = 78) bears and a mean density estimate of 23 bears/100 km^2 (Table 1.7; Appendix A).

Table 1.7: Black bear (*Ursus americanus*) population estimates using cameras and a space-to-event model bootstrapped 1,000 times by sampling from cameras with replacement. Density estimates represent combined data sources of motion-trigger photos and timelapse photos. Comparable density estimate ranges derived from Beecham and Rohlman 1994, Stetz et al. 2014, Loosen et al. 2019, Welfelt et al. 2019.

Study Area	Deployment Type	N	SD	Density (bears/100 km^2)	Within Comparable Range	N	SD	Density (bears/100 km^2)	Comparable Range
				2020				2021	
St. Joe	Random	218	53	8	0%	536	116	19 – 20	100%
St. Joe	Targeted	768	176	28 – 29	100%	131	51	5	0%
Clearwater	Random	388	136	9 – 10	0%	367	79	9	0%
Clearwater	Targeted	183	79	4 – 5	0%	98	43	2	0%
Council	Targeted	351	78	22 – 23	100%	224	68	14 – 15	100%

In 2021, STE bootstrapping abundance estimates for the St. Joe study area were 44% lower with 536 (SD = 116) bears and density estimates of 8 bears/100km^2 and 40% lower with 131 (SD = 51) bears and 5 bears/100 km^2 for random and targeted deployments, respectively. Clearwater study area abundance and density estimates decreased 44% and were 367 (SD = 79) bears and 9 bears/100 km^2 for random deployment and decreased 33% and were 98 (SD = 43) bears and 2 bears/100 km^2 for targeted deployment. Council abundance estimates decreased 41% and were 224 (SD = 68) bears and density estimates of 8 bears/100 km^2 (Table 7). Bootstrapped estimates from the STE model fell within the range of comparable density estimates in only 4 out of 10 (40%) comparisons (Table 7).

Discussion

There was no single combination of model, photo type, and camera deployment that produced consistent density estimates across all years or study areas. Due to the sensitivity of the TTE and STE models, there are several possible reasons for these inconsistent results. The TTE model appears most sensitive to violations of random camera placement, as evidenced by targeted camera deployments density estimates not comparing well and being higher than black bear density ranges from the literature. Targeted cameras also had a higher number of motion photographs per camera, often aided by the influence of cameras with a higher proportion of motion trigger photos. The STE model produced density estimates that were most comparable with those in the literature. These STE estimates, however, were often lower than the comparable density estimate ranges demonstrating the STE is highly dependent upon obtaining sufficient timelapse photographs of bears.

There was no consistency in the number of photos taken each year and within each study area. Different years and camera deployments had considerable differences in both the number of timelapse and motion photos. From 2020 to 2021, the random camera deployment from the St. Joe study area had a 200% increase in the number of timelapse photographs and an almost 250% increase in the number of motion photographs. The number of photos in the Clearwater study area followed a similar trend with random deployment photo increases, but targeted deployment cameras showed little change in the number of timelapse or motion photos between years.

Targeted deployments generally had a higher number of motion photographs per camera when compared to random deployments, likely due to the larger camera area surveyed without obstructions. This tendency of targeted cameras to have an increased number of motion trigger photos was echoed in several years by the random deployment cameras (ex. 2021 random deployments in the St. Joe and Clearwater study areas). Variability in detections per camera leads to certain cameras with a higher proportion of motion trigger photos, or 'outlier' cameras. When estimates were higher than comparable densities from the literature, there often tended to be several outlier cameras.

More effort is required to define what constitutes as an 'outlier' camera, whether it simply be a high number of counts or specific animals that stayed in the camera viewshed for an extended period. For example, the St. Joe study area's randomly deployed cameras in 2021 had a total of 2,086 motion trigger photos. Out of the 135 cameras containing count data within the deployment period, 74 of those had 0 motion photos of black bears. The five cameras with the highest number of motion trigger photos had 15%, 13%, 9%, 7%, and 5% of the total motion triggered photos. The remaining 58 cameras with motion triggered photos all contained 0.05 – 4% of the photos. Removing these five top percentage cameras reduced the TTE density estimates to 31 bears/100 km^2 (24 – 40, 95% CI) from 42 bears/100 km^2 (33 – 51, 95% CI), overlapping 94% with comparable densities from the literature (Beecham and Rohlman 1994, Stetz et al. 2014, Loosen et al. 2019, Welfelt et al. 2019). In this example, the camera with the highest percentage of photos (15%) was due to 6 groupings of photos where a bear stayed in the camera for an extended period instead of simply passing by. Based on these findings, a criterion could be set to remove cameras containing a percentage of the motion triggered photos over a certain threshold. Another possibility would be to extend the length between sampling occasions to reduce chances of an individual remaining in the viewshed and increasing the adherence to assumptions of independent observations.

Across all years (except the St. Joe and Clearwater study areas in 2020, and St. Joe in 2021), the TTE model had estimates that were higher than the comparable density range. An assumption for the TTE and STE models is random camera placement (Moeller et al. 2018). Violation of this assumption was echoed in our results that found targeted cameras tended to be as much as 1,300% over the highest comparable density estimates for each study area

(Beecham and Rohlman 1994, Stetz et al. 2014, Loosen et al. 2019, Welfelt et al. 2019). In some cases, bootstrapping the TTE reduced the density estimates from targeted cameras and yielded comparable density estimates to both the literature and the TTE estimate from randomly deployed cameras. More frequently, the TTE model estimates remained high post-bootstrapping, potentially due to outlier cameras still maintaining their strong effect on the overall estimate.

The single run estimates from the STE tended to overlap more than the TTE model with the comparable densities, regardless of camera deployment style. Since the STE only uses time trigger photos, there is no variation associated with individual camera motion trigger detections or a need for bear movement rates (Rowcliffe et al. 2011, Moeller et al. 2018). The placement of cameras showed no bias in the number of timelapse photographs taken. In our analysis, it was common for randomly deployed cameras to have a greater frequency of timelapse photographs of bears than targeted cameras, potentially due to a greater density of cameras than targeted deployment. Both the St. Joe and Clearwater study areas had a higher frequency of timelapse photographs of bears per random deployed camera than targeted camera in 2021. Despite the increase in number of timelapse photographs, the STE model density estimates were not biased high. STE estimates instead were still regularly lower than those estimates from the TTE models. Bootstrapping the STE model drove estimates even lower to unrealistic levels compared to the literature (Beecham and Rohlman 1994, Stetz et al. 2014, Loosen et al. 2019, Welfelt et al. 2019). These results were likely due to random sampling of cameras often losing the few cameras that did have timelapse photographs of bears.

These results demonstrate that the STE model is strongly dependent upon obtaining enough timelapse photos of black bears regardless of random or targeted camera deployment. In 2020, the Clearwater study area had few ($n < 6$) timelapse photos of black bears with both camera deployments and the STE model was not able to produce comparable estimates of density. In 2021, only the St. Joe study area had sufficient timelapse detections to produce comparable density estimates. While the estimates from the Council study area were within the range of comparable densities, estimates were considerably lower in 2021 than 2020. Given our lack of knowledge to any major changes in black bear abundance, there is little

evidence to support these drastic population drops. Including all data sources (timelapse and motion triggered photos) does increase the number of photographs available for analysis, however, with so few photos it does little to increase the overall density estimate. Widening the sample length can include more motion photographs in analysis, but introduces new biases and can inflate the density estimate (Loonam 2019). Sparse data coupled with the randomization of each run of the STE model (i.e., the order in which cameras are sampled), leads to varying estimates over each iteration.

Random deployment appears to be critical when using both the TTE and STE. However, obtaining enough timelapse photos is not guaranteed, even with a large-scale camera deployment. Increasing the density of cameras most likely would increase timelapse photos in either random or targeted deployment and increase the area in which density is calculated since the TTE and STE are simply calculating density for the camera areas surveyed. Future research could determine the minimum number of cameras required to produce accurate and precise estimates from timelapse photos. Additionally, motion photos from random deployed cameras can still be biased by 'outlier' cameras, the same issue that arises from targeted deployed cameras. Determining a criterion for outlier cameras (e.g., if animals are sleeping in front of cameras) would make the TTE and STE model function regardless of deployment style and could eliminate the need for a double camera deployment type (i.e., random and targeted) as used in our project.

Management Implications

Our research found that black bear density estimates are most comparable to density estimates from the literature and adhere most strictly to the assumptions of the TTE and STE when deploying cameras randomly. When deploying cameras randomly, however, we recommend increasing the number of cameras deployed over our sample sizes to increase the probability of obtaining enough timelapse photos of bears and area surveyed. Additionally, the length of the occasion can be increased to include more motion trigger photos, however, we do not recommend including all motion-trigger photos because it can bias estimates high. Finally, quantifying outlier cameras and determining the reason for the high frequency of photos (i.e., many animals vs. one animal resting in front of camera) will allow managers to

potentially remove or keep certain cameras in their analyses. Addressing the sensitivities of the STE and TTE models will make them more precise and reliable.

A bootstrapping process such as the one we used would also aid in the removal of undue bias from outlier cameras (e.g., cameras where images are not independent in time such as when an individual remains in the viewshed for multiple trigger events) and is generally recommended with the TTE model because of the high number of motion photos. We recommend removing cameras when an individual has rested for a period of time in the camera's viewshed. However, despite removal of outlier cameras and individuals remaining in the camera viewshed, the bootstrapped iterations of the time to event model tended to remain high (Appendix A). Additionally, bootstrapping the space to event model consistently biased estimates low (Appendix A). The variability in the bootstrapping process, while useful, does not necessarily mean that bootstrapping estimates is always the best course of action.

References

Amstrup, S. C., and J. Beecham. 1976. Activity patterns of radio-collared black bears in Idaho. The Journal of Wildlife Management 40:340–348.

Ausband, D. E., P. M. Lukacs, M. Hurley, S. Roberts, K. Strickfaden, and A. K. Moeller. 2022. Estimating wolf abundance from cameras. Ecosphere 13:1–8.

Beecham, J. J., and J. Rohlman. 1994. A shadow in the forest: Idaho's black bear. University of Idaho Press, Moscow, Idaho.

Beston, J. A., and R. D. Mace. 2012. What can harvest data tell us about Montana's black bears? Ursus 23:30–41.

Burton, A. C., E. Neilson, D. Moreira, A. Ladle, R. Steenweg, J. T. Fisher, E. Bayne, and S. Boutin. 2015. Wildlife camera trapping: A review and recommendations for linking surveys to ecological processes. Journal of Applied Ecology 52:675–685.

Chandler, R. B., and A. J. Royle. 2013. Spatially explicit models for inference about density in unmarked or partially marked populations. The Annals of Applied Statistics 7:936–954.

Coster, S. S., A. I. Kovach, P. J. Pekins, A. B. Cooper, and A. Timmins. 2011. Genetic mark-recapture population estimation in black bears and issues of scale. Journal of Wildlife Management 75:1128–1136.

Davis, M. L., J. Berkson, D. Steffen, and M. K. Tilton. 2007. Evaluation of Accuracy and Precision of Downing Population Reconstruction. Journal of Wildlife Management 71:2297.

Diefenbach, D. R., J. L. Laake, and G. L. Alt. 2004. Spatio-Temporal and Demographic Variation in the Harvest of Black Bears: Implications for Population Estimation. Journal of Wildlife Management 68:947–959.

Jackson, R. M., J. D. Roe, R. Wangchuk, and D. O. Hunter. 2006. Estimating Snow Leopard Population Abundance Using Photography and Capture–Recapture Techniques. Wildlife Society Bulletin 34:772–781.

Karanth, K. U. 1995. Estimating tiger Panthera tigris populations from camera-trap data using capture-recapture models. Biological Conservation 71:333–338.

Kasworm, W. F., and T. L. Manley. 1990. Road and Trail Influences on Grizzly Bears and Black Bears in Northwest Montana. Bears: Their Biology and Management 8:79–84.

Loonam, K. E. 2019. Assessing the Robustness of Time-to-Event Abundance Estimation Let us know how access to this document benefits you. Graduate Student Theses, Dissertations, & Professional Papers. 11477. <https://scholarworks.umt.edu/etd/11477>.

Loosen, A. E., A. T. Morehouse, and M. S. Boyce. 2019. Land tenure shapes black bear density and abundance on a multi-use landscape. Ecology and Evolution 9:73–89.

McCall, B. S., M. S. Mitchell, M. K. Schwartz, J. Hayden, S. A. Cushman, P. Zager, and W. F. Kasworm. 2013. Combined use of mark-recapture and genetic analyses reveals response of a black bear population to changes in food productivity. Journal of Wildlife Management 77:1572–1582.

Moeller, A. K., P. M. Lukacs, and J. S. Horne. 2018. Three novel methods to estimate abundance of unmarked animals using remote cameras. Ecosphere 9.

Mumma, M. A., C. Zieminski, T. K. Fuller, S. P. Mahoney, and L. P. Waits. 2015. Evaluating noninvasive genetic sampling techniques to estimate large carnivore abundance. Molecular Ecology Resources 15:1133–1144.

Parsons, A. W., T. Forrester, W. J. McShea, M. C. Baker-Whatton, J. J. Millspaugh, and R. Kays. 2017. Do occupancy or detection rates from camera traps reflect deer density? Journal of Mammalogy 98:1547–1557.

Roseberry, J. L., and A. Woolf. 1991. A Comparative Evaluation of Techniques for Analyzing White-Tailed Deer Harvest Data. Wildlife Monographs 117:3–59.

Rosenberry, C. S., D. R. Diefenbach, and B. D. Wallingford. 2004. Reporting-Rate Variability and Precision of White-Tailed Deer Harvest Estimates in Pennsylvania. Journal of Wildlife Management 68:860–869.

Rowcliffe, J. M., J. Field, S. T. Turvey, and C. Carbone. 2008. Estimating Animal Density

Using Camera Traps without the Need for Individual Recognition. Journal of Applied Ecology 45:1228–1236.

Rowcliffe, M. J., C. Carbone, P. A. Jansen, R. Kays, and B. Kranstauber. 2011. Quantifying the sensitivity of camera traps: An adapted distance sampling approach. Methods in Ecology and Evolution 2:464–476.

Rupp, S. P., W. B. Ballard, and M. C. Walace. 2000. A nationwide evaluation of deer hunter harvest survey techniques. Wildlife Society Bulletin 28:570–578. <https://www.jstor.org/stable/3783605%0Ahttp://www.scopus.com/scopus/inward/record.url?eid=2-s2.0-0033673422&partnerID=40>.

Stenglein, J. L., L. P. Waits, D. E. Ausband, P. Zager, and C. M. Mack. 2010. Efficient, Noninvasive Genetic Sampling for Monitoring Reintroduced Wolves. Journal of Wildlife Management 74:1050–1058.

Stetz, J. B., K. C. Kendall, and A. C. Macleod. 2014. Black bear density in glacier national park, montana. Wildlife Society Bulletin 38:60–70. Wildlife Society Bulletin.

Team, R. C. 2021. R: A language and environment for statistical computing. R Foundation for Statistical Computing, Vienna, Austria. <https://www.r-project.org/>.

Tilton, M. K. 2005. Evaluating the effectiveness of population reconstruction for black bear (Ursus americanus) and white-tailed deer (Odocoileus virginianus) population management. <http://vtechworks.lib.vt.edu/handle/10919/35455>.

Welfelt, L. S., R. A. Beausoleil, and R. B. Wielgus. 2019. Factors Associated with black bear density and implications for management. Journal of Wildlife Management 83:1527–1539. John Wiley & Sons, Ltd. <http://dx.doi.org/10.1002/jwmg.21744>.

Young, D. D., and J. J. Beecham. 1986. Black Bear Habitat Use at Priest Lake , Idaho. Bears: Their Biology and Management 6:73–80.

Chapter 2: Predicting Black Bear Population Trends Using Yearly Huckleberry Productivity

Introduction

One of the most critical variables of interest in wildlife population management is recruitment (Chandler et al. 2018). Obtaining yearly counts of young is feasible when a species is found in open landscapes but becomes increasingly difficult when animals are found in forested areas (Serrouya et al. 2017). Numerous methods and models have been developed to estimate recruitment and life-history of populations that would otherwise be difficult to study. Among these are the use of artificial breeding sites (Pilastro et al. 2003), capture-recapture techniques (Chandler et al. 2018), and more recently, camera surveys (Chitwood et al. 2017). Each of these techniques has its uses along with its own set of limitations.

Artificial breeding sites often miss animals that recruit in natural areas resulting in partial monitoring of the population (Pilastro et al. 2003). Capture-recapture methods, while used extensively in wildlife management has similar restrictions in that it is often representative of only a small subpopulation (Chandler et al. 2018). The time, effort, and funding necessary for an intensive capture-recapture project is also prohibitive for many organizations to do for an extended period of time if at all (Mumma et al. 2015). The use of passive detectors such as motion triggered trail cameras has significantly decreased the cost (after initial investment) and personnel required for abundance estimates (Karanth 1995, Rowcliffe et al. 2008, Parsons et al. 2017) but the application of passive detectors to estimating recruitment is relatively new and fraught with its own issues. An actual measure

of recruitment can only be estimated when getting a percentage of females with young and only applicable when there are clear difference between males and females of the species such as white-tailed deer (*Odocoileus virginianus;* Chitwood et al. 2017).

Food availability is often a limiting factor for both wildlife and fish species, affecting both survival rates and recruitment. Quantifying the relationship between food availability and recruitment could be a strong step toward estimating population trends when the amount of available food is quantifiable. The American black bear (*Ursus americanus*) is one such species in which fecundity, and subsequently recruitment, can be highly variable depending on yearly variations in habitat productivity and mast abundance (Beston and Mace 2012). In practically every region they are found, black bears rely on a fall mast to gain enough weight for overwintering survival and reproduction (Eiler et al. 1989). Black bear fecundity is highly subject to variation in habitat productivity as females must reach a certain weight capable of supporting cubs or implantation can be halted and fertilized eggs rejected (Beston 2011). The fecundity and survival of black bears differs between the eastern and western portions of their range in the United States (Beston 2011). Eastern black bears benefit from a longer growing season and more nutritious hard mast resulting in greater fecundity but lower adult survival; western black bears (particularly in the northwest) rely on soft mast and have a much shorter growing season, leading to lower fecundity but higher adult survival (Beston 2011).

In Idaho, black bears rely heavily on the late summer huckleberry crop in preparation for their winter denning. Availability of berries and other forage in the fall affects black bear weights before denning when low, but can also delay denning in years when food is abundant (Reynolds and Beecham 1980). Black bear fecundity also follows the general trend of other

western bears, having low fecundity but higher adult survival rates. Years of lower mast and berry crop abundance have been correlated with lower fall weights for bears that lead to decreased recruitment and survival of cubs (Rogers 1976, Eiler et al. 1989, Costello et al. 2003). The heavy reliance of black bears on huckleberry crops can affect yearly population trends, particularly due to the immense variation that environmental effects can have on huckleberry crops.

The reliance of black bears on huckleberries for both overwintering and survival and recruitment suggests that population trends for the following year could be estimated were huckleberry abundance quantified. Previous studies have predicted the presence and abundance of huckleberries to relate to black bear and grizzly bear (*U. arctos*) recruitment (Holden et al. 2012, Proctor et al. 2018), however, these studies were catered to specific regions and not generalizable to Idaho. Therefore, we aimed to create a simple huckleberry productivity model that could then be related to black bear abundance between years. We hypothesized that environmental variables such as precipitation and canopy cover would be significant predictors of huckleberry abundance. We also hypothesized that increased huckleberry productivity would result in increased black bear recruitment the following year.

Methods

Study Areas

The study areas for my project were selected by the Idaho Department of Fish and Game (IDFG) across three different regions (Panhandle, Clearwater, and Southwest) and consisted of a Game Management Unit as the study area in each region: GMUs 6, 10A, and 32A, respectively (Fig. 1.1). The most northern of these units, GMU 6 (hereafter St. Joe

study area), is 2,726 km^2. Around 40% of the unit is managed by the U.S. Forest Service (USFS) within the St. Joe National Forest and is a frequented location for summer recreation. The reaming land contains 40% privately owned land (largely by the logging company PotlatchDeltic), 10% state of Idaho, and 10% split between BLM and Bureau of Indian Affairs. The area is notably a more Pacific climate and lower elevation than areas in southern Idaho but consists of steep slopes created by streams. Areas that are unlogged consist of cedar (*Cedrus* spp.), hemlock (*Tsuga* spp.), and pine (*Pinus* spp.) below the treeline with mountain hemlock (*Tsuga mertensiana*), subalpine fir (*Abies lasiocarpa*), Engelmann spruce (*Picea engelmannii*), and whitebark pine (*Pinus albicaulis*) occurring around and near the treeline.

The largest of the three study areas, GMU 10A (Clearwater study area), is 4,028 km^2. Approximately 50% of the unit consists of private land, 24% USFS managed land within the Nez Perce-Clearwater National Forest, and 24% State of Idaho Managed Land. The area north of the Dworshak Reservoir is of a similar climate and species makeup as that of the St. Joe study area. South of the Reservoir, the area within the Nez Perce-Clearwater National Forest is a transition stage to drier forests and typically lacks the hemlocks found in the northern half. Additionally, the area in the southwestern portion of the unit around Orofino, ID and along the Clearwater River are much warmer and drier with an overstory of Douglas-fir (*Pseudotsuga menziesii*) and ponderosa pine (*Pinus ponderosa*) forest and open grassy areas that are typically livestock grazed and hay farmed.

GMU 32A (Council study area) is the southernmost unit of the project and the smallest study area t 1,545km^2. The northwestern portion of the unit is bordered by Hwy. 95 and stretches south to Banks, ID containing the East Fork Weiser River and the Middle Fork

Weiser River. GMU 32A is majority public land (70%) with the eastern two-thirds consisting of the Payette National Forest and a small section of Boise National Forest (58%). The remaining public land occurs on the western side and is a mixture of BLM (9%) and State of Idaho Land (3%) intermixed with private land. At higher elevations the area is dominated by alpine meadows, rocky soils and jagged peaks. The areas immediately surrounding these tend to be more mesic and have an overstory of subalpine fir, lodgepole pine (*Pinus contorta*), whitebark pine, mountain hemlock, and alpine larch (*Larix lyallii*). Huckleberry shrubs are most likely to be found in these more mesic areas than in the surrounding drier zones. When not in the immediate vicinity of these zones, ponderosa pine is dominant. West of the mountain ranges, the GMU is dominated by sagebrush (*Artemisia* spp.) and grasses and primarily used for livestock grazing. During mid- to late-summer months, the entire unit is used for cattle grazing as part of grazing permits and allotments.

Field Methods & Analysis

Huckleberry Sampling

We used a model predicting various shrub species in Idaho developed by IDFG (unpublished data) in 2020 and 2021. We randomly selected potential huckleberry shrub locations to visit from over 1 million predicted sites. Our transect survey protocols were loosely based on those developed by Holden et al. (2012). We identified a patch suitable for survey when there were continuous huckleberry shrubs in 25 meters in any direction. To begin our survey, a random azimuth was selected through the densest patch of *Vaccinium* spp. available and ran a measuring tape through the patch from 25 – 30 meters. Using a 0.04 m^2 quadrat and a starting location of 0 m, we counted all ripe and unripe berries (not

including failed berries) within the quadrat. We advanced the measuring tape at intervals of 0.5 meters with quadrats containing less than 50% huckleberry shrub recorded as NA and the quadrat moved forward. We repeated the survey process until 50 quadrats containing huckleberry shrubs had been surveyed. Additionally, we recorded the overstory cover, elevation, and habitat type for each transect plot and a qualitative assessment of overall shrub health in each quadrat.

Calculating Bear Abundances

We initially ran a time to event and space to event model on black bear cub photos to predict abundance, but results varied widely and were not realistic for the population estimates of the study areas. We also attempted to use a black bear cub index of cubs/trap night but lacked sufficient data to do so. Alternatively, we opted to create an index of bear abundances that was a function of bears/trap night. To obtain an index of bear abundances for comparisons between years, we used black bear photos (adult and cubs) obtained from targeted deployment cameras (i.e., along roads and trails) due to that deployment style begin used in all three study areas throughout the two years. Bears/trap night was established using the analyzed range of camera abundances for each year and study area (e.g., June 1 – Aug. 31 for 2020 in the St. Joe and Clearwater study area). We used a Pearson correlation to test whether estimated huckleberry abundance in year t (2020) was correlated with bears/trap night in year t+1 (2021).

Model Analysis

We initially included nine variables in our huckleberry predictive model: mean temperature from December (of the previous year) to March, mean temperature from April to July, total precipitation from December (of the previous year) to March, total precipitation from April to July (PRISM Climate Group 2022), canopy cover, aspect (0 – 360°), slope, elevation, and soil type (14 soil types; gSSURGO 2020). We also included an interaction term between mean temperature and canopy cover to account for shading during extreme temperatures. A histogram of the data showed that our transect totals were highly zero-inflated, leading us to pursue a zero-inflated Poisson and a zero-inflated negative binomial regression. We scaled all variables to a z-scale due to measurement types differing between each covariate. To determine whether to use a zero-inflated Poisson or a zero-inflated negative binomial regression, we compared models containing all covariates and compared Akaike information criterion estimator corrected for small sample size (AICc) scores between the two models (Zuur et al. 2009).

After selecting the type of model to use, we dropped terms sequentially based on the covariate with the highest p-value after each model iteration. We also used a likelihood ratio test to compare each model with the dropped term to the model that included all variables. To validate the models, we plotted Pearson residuals against the fitted values, each explanatory variable, and the original data versus the fitted data in the count model to ensure they formed a straight line. Additionally, we took the predicted data and plotted the probability of zeroes (including false zeroes) for a range of values of each predictive covariate.

Results

Huckleberry Surveys

Using the IDFG huckleberry predictive model we surveyed 120 sites in 2020 and 200 sites in 2021 (Table 2.1). The total number of berries counted in 2020 was 11,472 and 17,879 in 2021.

Table 2.1: Total number of huckleberry (*Vaccinium* spp.) transects surveyed in Idaho, USA, 2020 – 2021. Transect totals from surveys were used to determine which environmental variables were effective in predicting total huckleberry productivity.

Study Areas	2020			2021		
	No. of Transects	Total Huckleberries	$\bar{x}$ Berries/Transect	No. of Transects	Total Huckleberries	$\bar{x}$ Berries/ Transect
St. Joe	50	6,864	137.28	71	9,122	128.48
Clearwater	46	3,088	67.13	74	3,544	47.89
Council	20	1,520	76	46	5,213	113.33
Total	116	11,472	98.90	191	17,879	93.61

Model Analysis

Mean temperature between December and March and mean temperature between April and July were highly correlated in both 2020 and 2021 (0.73, 0.64). Therefore, we combined these two covariates into a single covariate of mean temperature between December and July. Total precipitation in December through March and total precipitation in April through July were highly correlated in 2020 (0.83), so we combined these values into a single covariate of total precipitation in December through July. Total precipitation between these two ranges were not correlated in 2021.

Our initial comparisons of a zero-inflated Poisson and zero-inflated negative binomial found that positive transect totals were not Poisson distributed, with the zero-inflated Poisson producing an Akaike information criterion estimator corrected for small sample size (AICc) of 8,944 and an AICc of 1,297 when using the negative binomial in 2020. The AICc for the zero-inflated Poisson in 2021 was 20,603 and the AICc for the zero-inflated negative binomial was 2,031. Therefore, we used a zero-inflated negative binomial model for both years.

We dropped terms sequentially based on the highest p-value after each model iteration, regardless of count or zero model. Significant environmental covariates in 2020 for the count model were mean temperature between December and July and canopy cover along with an interaction term between the two. For the zero model only mean temperature between December and July was significant (Table 1.2). This model was most supported of all tested models and when compared to an intercept only null model (ΔAICc = 21). In 2021, the significant covariates for the count model included mean temperature between December and July, canopy cover, and the addition of aspect and elevation. The zero model had significant covariates of canopy cover and elevation (Table 2.3). The model was most supported out of all models including the intercept only null model (ΔAICc = 64).

The total number of bears per trap night for 2020 in the St. Joe study area was 0.188 bears/trap night, 0.149 bears/trap night in the Clearwater study area, and 0.422 bears/trap night in the Council study area. In 2021, the number of bears/trap night was 0.22 bears/trap night in the St. Joe study area, 0.207 bears/trap night in the Clearwater study area, and 0.489 bears/trap night in the Council study area (Table 2.4). We found that the mean transect totals for each unit in 2020 were not correlated with bears/trap night in 2021 (Pearson's r = -0.165).

Table 2.2: Zero-inflated negative binomial model (ZINB) analysis of environmental and climatic variables that affect huckleberry productivity in three study areas of Idaho, USA, 2020. The variables included were mean temperature between December and July, total precipitation between December and July, canopy cover, slope, aspect, elevation, soil type, and an interaction term between mean temperature between December and July and canopy cover. Covariates to the right of the bar are the covariates used in the zero portion of the ZINB model.

Model	k	LogLik	AICc	ΔAICc
Transect Totals ~ MeanTemp + Canopy Cover + MeanTemp*CanopyCover | MeanTemp	4	-672.2	1,269	0
Transect Totals ~ Mean Temp + Canopy Cover + Mean Temp*Canopy Cover | Mean Temp + Canopy Cover	5	-627.2	1,272	3
Transect Totals ~ Mean Temp + Canopy Cover + Mean Temp*Canopy Cover | Mean Temp + Canopy Cover + Mean Temp*Canopy Cover	6	-626.5	1,272	3
Transect Totals ~ Mean Temp + Canopy Cover + Mean Temp*Canopy Cover + Aspect | Mean Temp + Canopy Cover + Mean Temp*Canopy Cover	7	-626.0	1,274	5
Transect Totals ~ Mean Temp + Canopy Cover + Mean Temp*Canopy Cover + Aspect + Slope | Mean Temp + Canopy Cover + Mean Temp*Canopy Cover	8	-625.4	1,275	6
Transect Totals ~ Mean Temp + Canopy Cover + Mean Temp*Canopy Cover + Aspect + Slope + Elevation | Mean Temp + Canopy Cover + Mean Temp*Canopy Cover	9	-625.0	1,278	9
Transect Totals ~ Mean Temp + Canopy Cover + Mean Temp*Canopy Cover + Aspect + Slope + Elevation | Mean Temp + Canopy Cover + Mean Temp*Canopy Cover + Precip	10	-624.7	1,279	11

Transect Totals ~ Mean Temp + Canopy Cover + Mean Temp*Canopy Cover + Aspect + Slope + Elevation | Mean Temp + Canopy Cover + Mean Temp*Canopy Cover + Precip + Aspect	11	-624.4	1,281	13
Transect Totals ~ Mean Temp + Canopy Cover + Mean Temp*Canopy Cover + Aspect + Slope + Elevation | Mean Temp + Canopy Cover + Mean Temp*Canopy Cover + Precip + Aspect + Elevation	12	-624.2	1,283	15
Transect Totals ~ Mean Temp + Canopy Cover + Mean Temp*Canopy Cover + Aspect + Slope + Elevation | Mean Temp + Canopy Cover + Mean Temp*Canopy Cover + Precip + Aspect + Elevation + Slope	13	-623.7	1,285	17
Transect Totals ~ Mean Temp + Canopy Cover + Mean Temp*Canopy Cover + Aspect + Slope + Elevation + Soil Type | Mean Temp + Canopy Cover + Mean Temp*Canopy Cover + Precip + Aspect + Elevation + Slope	14	-623.6	1,287	19
(Null Model) Transect Totals ~ 1 | 1	1	-641.5	1,289	21
Transect Totals ~ Mean Temp + Canopy Cover + Mean Temp*Canopy Cover + Aspect + Slope + Elevation + Soil Type + Precip | Mean Temp + Canopy Cover + Mean Temp*Canopy Cover + Precip + Aspect + Elevation + Slope	15	-623.4	1,290	22
Transect Totals ~ Mean Temp + Canopy Cover + Mean Temp*Canopy Cover + Aspect + Slope + Elevation + Soil Type + Precip | Mean Temp + Canopy Cover	16	-623.3	1,293	24

+ Mean Temp*Canopy Cover + Precip + Aspect + Elevation + Slope + Soil Type

Table 2.3: Zero-inflated negative binomial model (ZINB) analysis of environmental and climatic variables that affect huckleberry productivity in three study areas of Idaho, USA, 2021. The variables included were mean temperature between December and July, total precipitation between December and March and April and July, canopy cover, slope, aspect, elevation, soil type, and an interaction term between mean temperature between December and July and canopy cover. Covariates to the right of the bar are covariates used in the zero portion of the ZINB model.

Model	k	LogLik	AICc	ΔAICc
Transect Totals ~ Mean Temp + Canopy Cover + Aspect + Elevation | Canopy Cover + Elevation + Aspect	6	-998.4	2,018	0
Transect Totals ~ Mean Temp + Canopy Cover + Aspect + Elevation | Canopy Cover + Elevation + Aspect + Precip (Apr. – Jul.) + Precip (Dec. – Mar.)	8	-997.3	2,020	2
Transect Totals ~ Mean Temp + Canopy Cover + Aspect + Elevation | Canopy Cover + Elevation + Aspect + Precip (Apr. – Jul.)	7	-998.8	2,021	3
Transect Totals ~ Mean Temp + Canopy Cover + Aspect + Elevation + Slope | Canopy Cover + Elevation + Aspect + Precip (Apr. – Jul.) + Precip (Dec. – Mar.)	9	-996.2	2,021	3
Transect Totals ~ Mean Temp + Canopy Cover + Aspect + Elevation + Slope + Soil | Canopy Cover + Elevation + Aspect + Precip (Apr. – Jul.) + Precip (Dec. – Mar.)	10	-996.2	2,023	5

Transect Totals ~ Mean Temp + Canopy Cover + Aspect + Elevation + Slope + Soil + Precip (Dec. – Mar.) | Canopy Cover + Elevation + Aspect + Precip (Apr. – Jul.) + Precip (Dec. – Mar.)	11	-996.1	2,025	7
Transect Totals ~ Mean Temp + Canopy Cover + Aspect + Elevation + Slope + Soil + Precip (Dec. – Mar.) | Canopy Cover + Elevation + Aspect + Precip (Apr. – Jul.) + Precip (Dec. – Mar.) + Slope	12	-996.1	2,027	9
Transect Totals ~ Mean Temp + Canopy Cover + Aspect + Elevation + Slope + Soil + Precip (Dec. – Mar.) | Canopy Cover + Elevation + Aspect + Precip (Apr. – Jul.) + Precip (Dec. – Mar.) + Slope + Mean Temp	13	-996	2,030	12
Transect Totals ~ Mean Temp + Canopy Cover + Aspect + Elevation + Slope + Soil + Precip (Dec. – Mar.) + Precip (Apr. – Jul.) | Canopy Cover + Elevation + Aspect + Precip (Apr. – Jul.) + Precip (Dec. – Mar.) + Slope + Mean Temp	14	-996	2,032	14
Transect Totals ~ Mean Temp + Canopy Cover + Aspect + Elevation + Slope + Soil + Precip (Dec. – Mar.) + Precip (Apr. – Jul.) | Canopy Cover + Elevation + Aspect + Precip (Apr. – Jul.) + Precip (Dec. – Mar.) + Slope + Mean Temp + Soil	15	-996	2,034	16
(Null model) Transect Totals ~ 1 | 1	1	-1038	2,082	64

Table 2.4: Total number of trap nights and motion triggered photos of bears from a targeted camera deployment in three study areas in Idaho, USA, 2020 – 2021.

	2020			2021		
Study area	Trap Nights	Motion Trigger Bear Photos	Bears/Trap Night	Trap Nights	Motion Trigger Bear Photos	Bears/Trap Night
St. Joe	5,050	949	0.188	4,303	949	0.221
Clearwater	5,441	808	0.149	4,508	933	0.207
Council	3,738	1,579	0.422	4,802	2,347	0.489

Discussion

The most supported model for predicting huckleberry abundance was not identical between years. The interaction term between mean temperature and canopy cover was not included in the 2021 model, but aspect and elevation were. The top model in each year, however, had much more support than both an intercept only null model and a model containing all environmental covariates suggesting good predictive ability. We found support that increasing canopy cover would negatively affect huckleberry productivity. Total precipitation was not significant in either year. In 2020, huckleberry productivity was negatively correlated with mean temperature which has been found in other studies of huckleberry productivity (Holden et al. 2012). Conversely the mean temperature (December to July) in 2021 was positively correlated with huckleberry productivity.

Mean temperatures were extremely different between 2020 and 2021. Mean temperatures (including day and night temperatures) were 25% higher in 2021 than 2020. This drastic increase in mean temperature follows with future climatic predictors of huckleberry ranges that expect huckleberry shrubs at higher elevations to be more productive as they escape withering from extreme heat (Prevéy et al. 2020). Additionally, this could be the potential cause for why elevation and aspect were included as significant covariates in the 2021 model as higher elevation transects and those on north facing slopes were more likely to escape high heat events and produce more berries. The coefficient values from our models in both years seem to support this hypothesis as mean temperature had a strong negative effect on huckleberry productivity in 2020 ($\beta = -0.26$) and elevation had a strong positive effect on huckleberry productivity in 2021 ($\beta = 0.788$). Aspect also had a positive correlation with huckleberry productivity in 2021 (e.g., north facing slopes; $\beta = 0.194$; Table 5).

Table 2.5: Coefficients (β) and p-values from top models (i.e., zero-inflated negative binomial) using environmental and climatic variables to predict huckleberry productivity in three study areas of Idaho, USA, 2020 and 2021.

Covariate	β	SE	P
2020			
Intercept	4.54	0.095	< 0.0001
Mean Temperature (Dec. – Jul.)	-0.338	0.100	< 0.0007
Canopy Cover	-0.317	0.115	0.006
Mean Temperature (Dec. – Jul.) * Canopy Cover	-0.260	0.113	0.22
2021			
Intercept	4.33	0.082	< 0.0001
Mean Temperature (Dec. – Jul.)	0.357	0.104	0.0006
Canopy Cover	-0.218	0.092	0.017
Aspect	0.194	0.080	0.016
Elevation	0.788	0.107	< 0.0001

While we attempted to test the predictive capabilities of our huckleberry models for black bear abundances, the mean transect totals in 2020 were not strongly correlated (r = -0.165) with our bear abundance index in 2021. Possible reasons for this are the variability in detection and motion trigger photographs (Rowcliffe et al. 2008). Future research should attempt to quantify a baseline for numbers of berries in a 'good' huckleberry year. Our means for total number of huckleberries were similar each year with averages of 98.90 (SD = 105.5) and 93.61 (SD = 137.8) in 2020 and 2021, respectively (Table 1). Additional years of huckleberry transect surveys would establish varying years of huckleberry abundance. Due to

similar means of transects in both years we were not able to adequately predict black bear abundances based on changes in huckleberry productivity. We note that our correlation test used just three data points. Although we did not find a strong correlation between huckleberry productivity and an index of bear abundance, it does not mean one does not exist. More years of sampling are necessary to adequately test for a relationship between vegetation productivity and bear abundance.

Other huckleberry models have been constructed to predict the environmental variables critical to huckleberry patch occurrence (Holden et al. 2012, Proctor et al. 2018, Prevéy et al. 2020). These occurrence models found similar covariates affecting patch occurrence such as canopy cover, which was found to be a significant covariate in our productivity model. However, the occurrence models from the literature did not attempt to predict huckleberry crop productivity trends and attempts to expand the model into the United States from British Columbia, Canada, were unsuccessful (Proctor et al. 2018, personal correspondence). Our goal was to create a portable and generalizable model that could predict huckleberry productivity based on a few key predictive variables. Although our top models were not identical in 2020 and 2021, there was overlap between the models suggesting some covariates (i.e., canopy cover, mean temperature) would be strongly predictive across years. There was little variation in bear detections or fruit abundances between years in our study limiting our ability to test for a relationship between vegetation and bear abundance.

We would recommend a more extensive survey containing more transects that are surveyed at different times of the growing season as fruiting is variable dependent upon elevation and aspect (Anzinger 2002). Future models should also obtain sufficient transect

plots to have a separate set of data to test model fit. The environmental variables we found to be significant covariates in our models were found in other studies on huckleberry productivity and should remain influential in future years of research (Anzinger 2002, Holden et al. 2012, Prevéy et al. 2020).

References

Anzinger, D. L. 2002. Big huckleberry (*Vaccinium membranaceum Dougl.*) ecology and forest succession, Mt. Hood National Forest and Warm Springs Indian Reservation, Oregon. Oregon State University Theses.

Beston, J. A. 2011. Variation in Life History and Demography of the American Black Bear. The Journal of Wildlife Management 75:1588–1596.

Beston, J. A., and R. D. Mace. 2012. What can harvest data tell us about Montana's black bears? Ursus 23:30–41.

Chandler, R. B., K. Engebretsen, M. J. Cherry, E. P. Garrison, and K. V. Miller. 2018. Estimating recruitment from capture-recapture data by modelling spatio-temporal varation in birth and age-specific survival rates. Methods in Ecology and Evolution 9:2115–2130. <https://doi.org/10.1111/2041-210X.13068>.

Chitwood, M. C., M. A. Lashley, J. C. Kilgo, M. J. Cherry, L. M. Conner, M. Vukovich, H. S. Ray, C. Ruth, R. J. Warren, C. S. Deperno, and C. E. Moorman. 2017. Are camera surveys useful for assessing recruitment in white-tailed deer? Wildlife Biology 2017.

Costello, C. M., D. E. Jones, R. M. Inman, K. H. Inman, C. Thompson, and H. B. Quigley. 2003. Relationship of Variable Mast Production to American Black Bear Reproductive Parameters in New Mexico. 14:1–16.

Eiler, J. H., G. W. Wathen, and M. R. Pelton. 1989. Reproduction in Black Bears in the Southern Appalachian Mountains. The Journal of Wildlife Management 53:353–360.

Holden, Z. A., W. F. Kasworm, C. Servheen, B. Hahn, and S. Dobrowski. 2012. Sensitivity

of berry productivity to climatic variation in the cabinet-yaak grizzly bear recovery zone, Northwest United States, 1989-2010. Wildlife Society Bulletin 36:226–231.

Karanth, K. U. 1995. Estimating tiger Panthera tigris populations from camera-trap data using capture-recapture models. Biological Conservation 71:333–338.

Mumma, M. A., C. Zieminski, T. K. Fuller, S. P. Mahoney, and L. P. Waits. 2015. Evaluating noninvasive genetic sampling techniques to estimate large carnivore abundance. Molecular Ecology Resources 15:1133–1144.

Parsons, A. W., T. Forrester, W. J. McShea, M. C. Baker-Whatton, J. J. Millspaugh, and R. Kays. 2017. Do occupancy or detection rates from camera traps reflect deer density? Journal of Mammalogy 98:1547–1557.

Pilastro, A., G. Tavecchia, and G. Marin. 2003. Long living and reproduction skipping in the fat dormouse. Ecology 84:1784–1792.

Prevéy, J. S., L. E. Parker, C. A. Harrington, C. T. Lamb, and M. F. Proctor. 2020. Climate change shifts in habitat suitability and phenology of huckleberry (Vaccinium membranaceum). Agricultural and Forest Meteorology 280:107803. Elsevier. <https://doi.org/10.1016/j.agrformet.2019.107803>.

Proctor, M., C. Lamb, and G. MacHutchon. 2018. Predicting grizzly bear food - Huckleberries - across the Columbia Basin. Habitat Conservation Trust Foundation.

Reynolds, D. G., and J. J. Beecham. 1980. Home Range Activities and Reproduction of Black Bears in West-Central Idaho. Bears: Their Biology and Management 181–190.

Rogers, L. 1976. Effects of mast and berry crop failures on survival, growth, and

reproductive success of black bears. Transactions of the 41st North American Wildlife and Natural Resources Conference 431–438.

Rowcliffe, J. M., J. Field, S. T. Turvey, and C. Carbone. 2008. Estimating Animal Density Using Camera Traps without the Need for Individual Recognition. Journal of Applied Ecology 45:1228–1236.

Serrouya, R., S. Gilbert, R. S. McNay, B. N. Mclellan, D. C. Heard, D. R. Seip, and S. Boutin. 2017. Comparing population growth rates between census and recruitment-mortality models. Journal of Wildlife Management 81:297–305.

Zuur, A. F., E. N. Ieno, N. J. Walker, A. A. Saveliev, and G. M. Smith. 2009. Mixed Effects Models and Extensions in Ecology with R

Appendix A

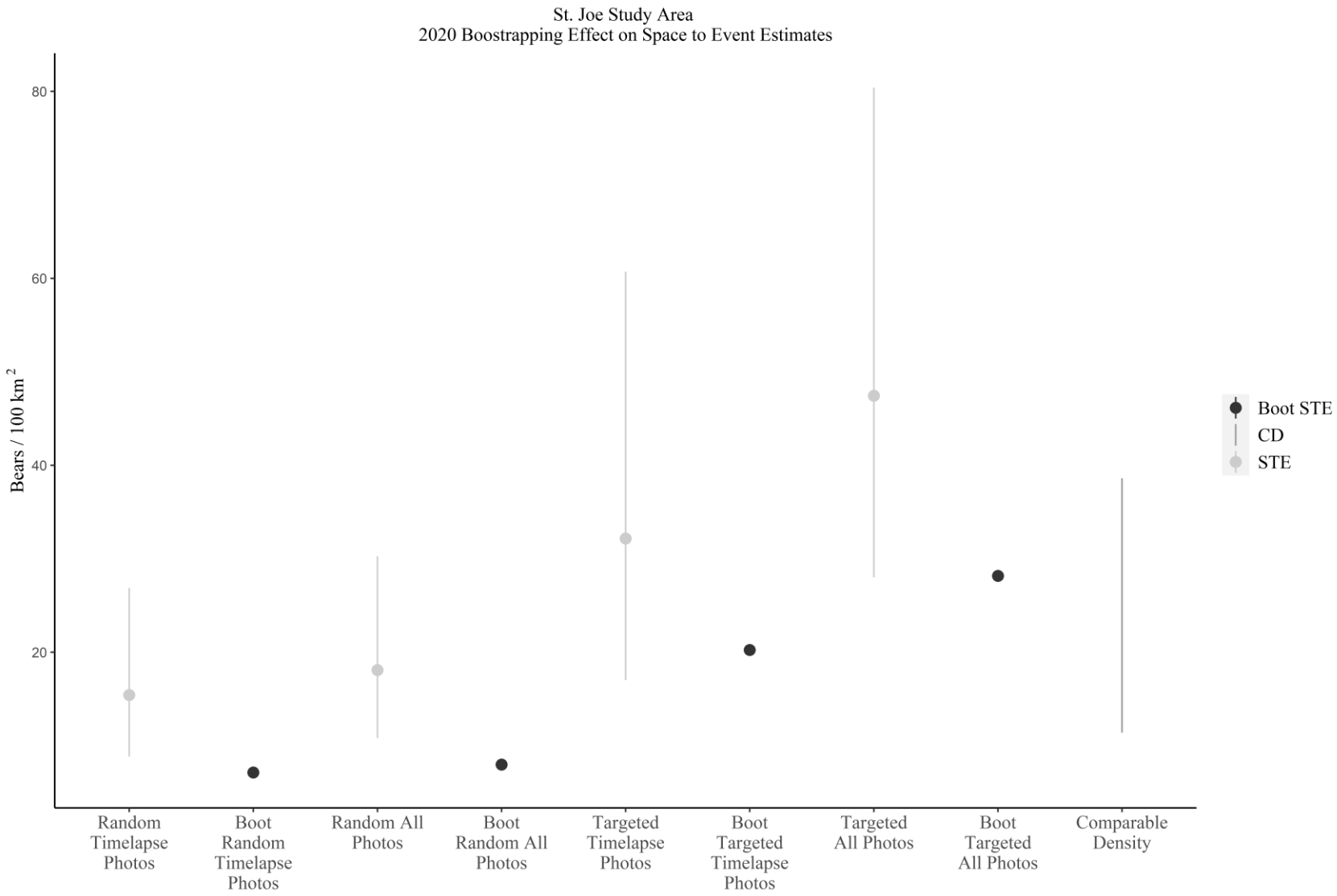

Figure A.1: The effect of bootstrapping on the space to event estimates in the St. Joe study area (2,727 km^2), Idaho, USA, 2020.

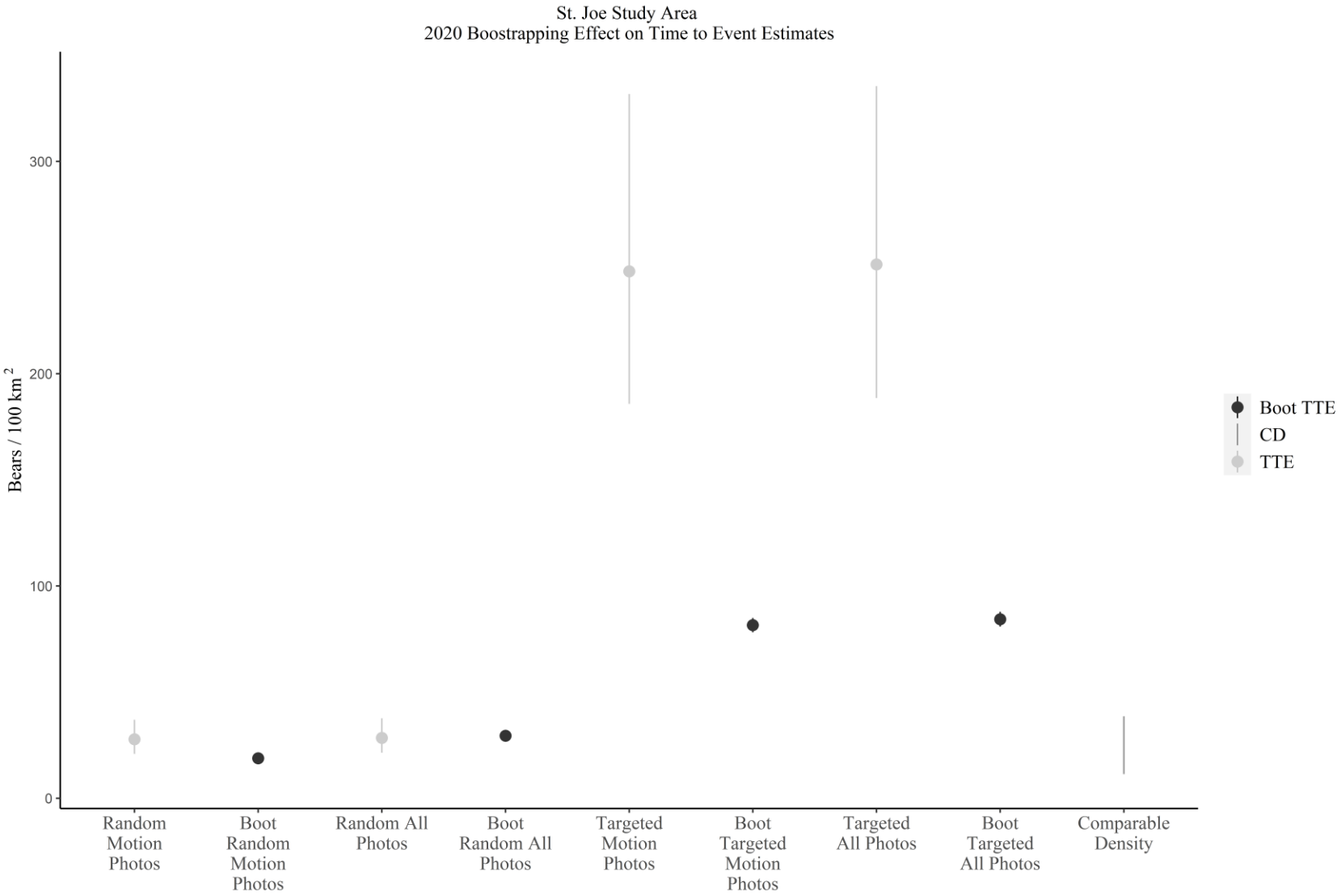

Figure A.2: The effect of bootstrapping on the time to event estimates in the St. Joe study area (2,727 km^2), Idaho, USA, 2020.

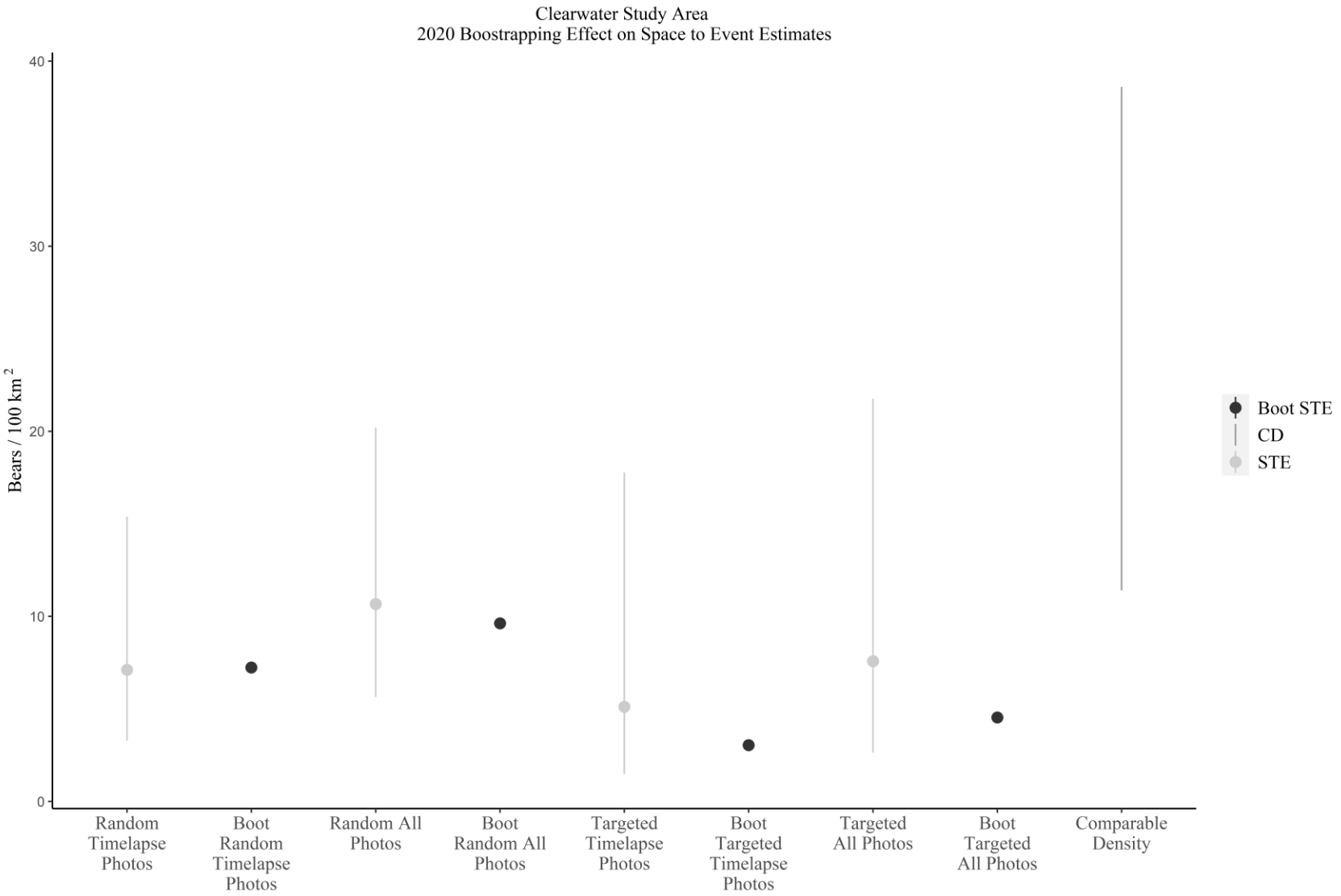

Figure A.3: The effect of bootstrapping on the space to event estimates in the Clearwater Study Area (4,029 km^2), Idaho, USA, 2020.

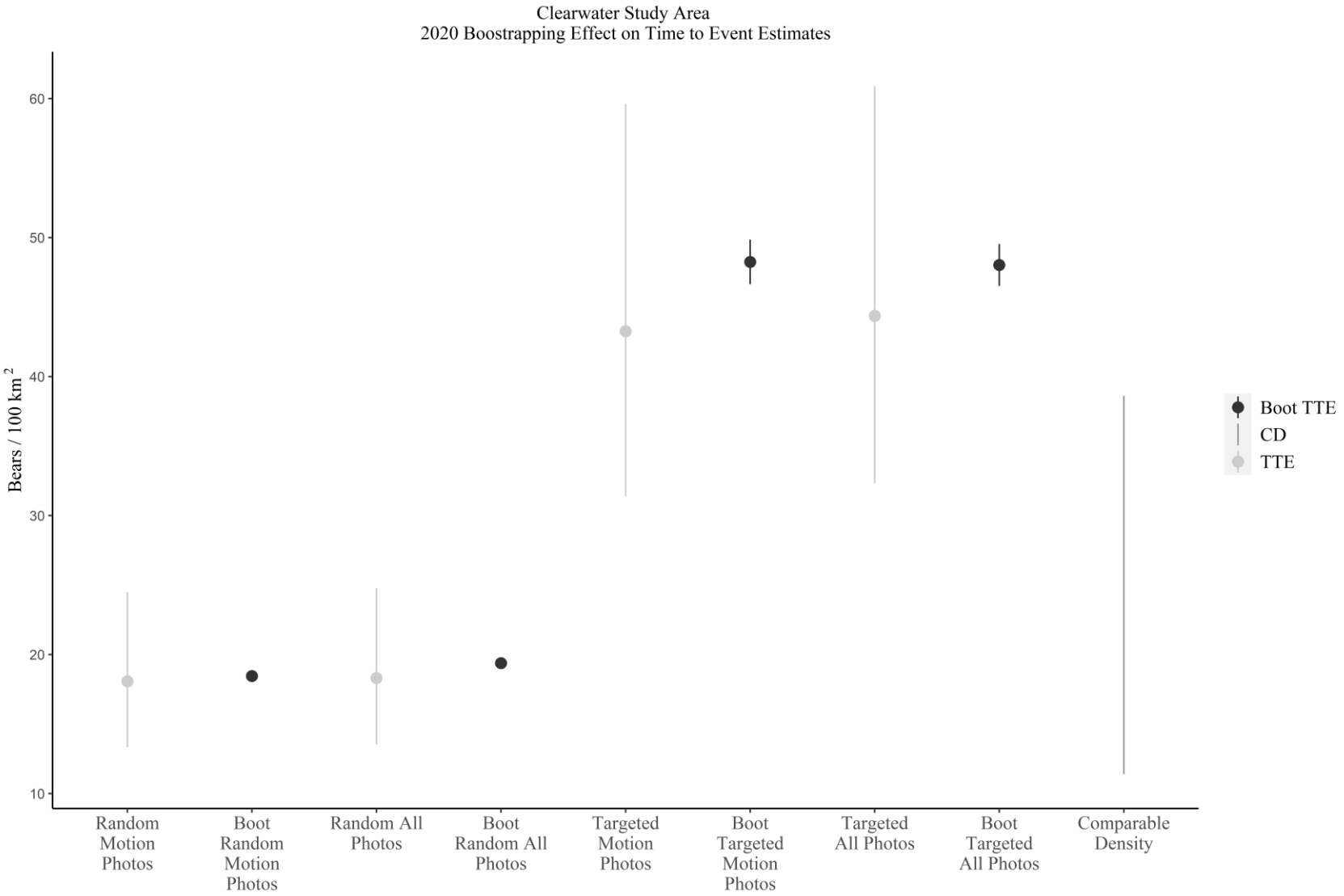

Figure A.4: The effect of bootstrapping on the time to event estimates in the Clearwater Study Area (4,029 km^2), Idaho, USA, 2020.

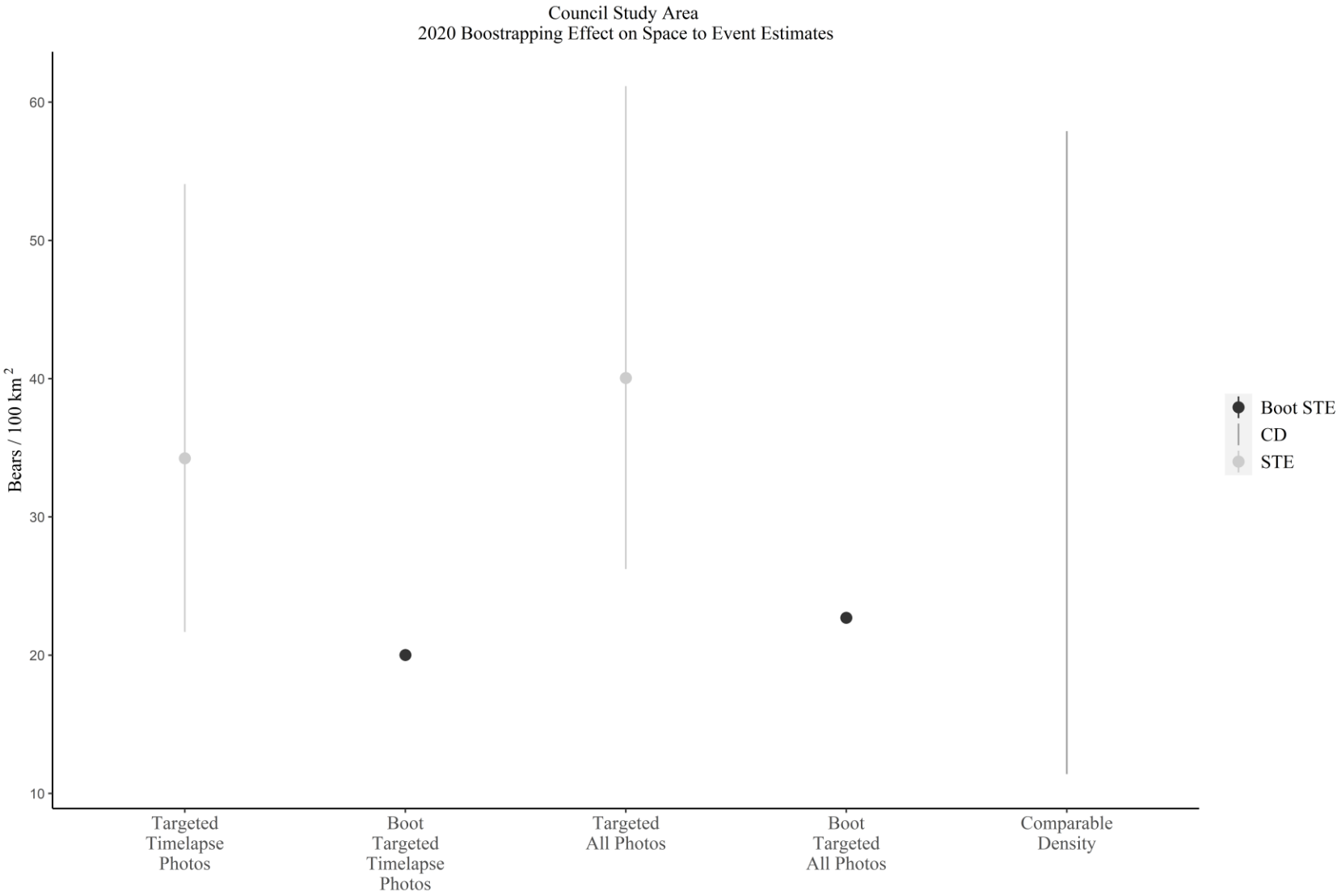

Figure A.5: The effect of bootstrapping on the space to event estimates in the Council study area (1,546 km^2), Idaho, USA, 2020.

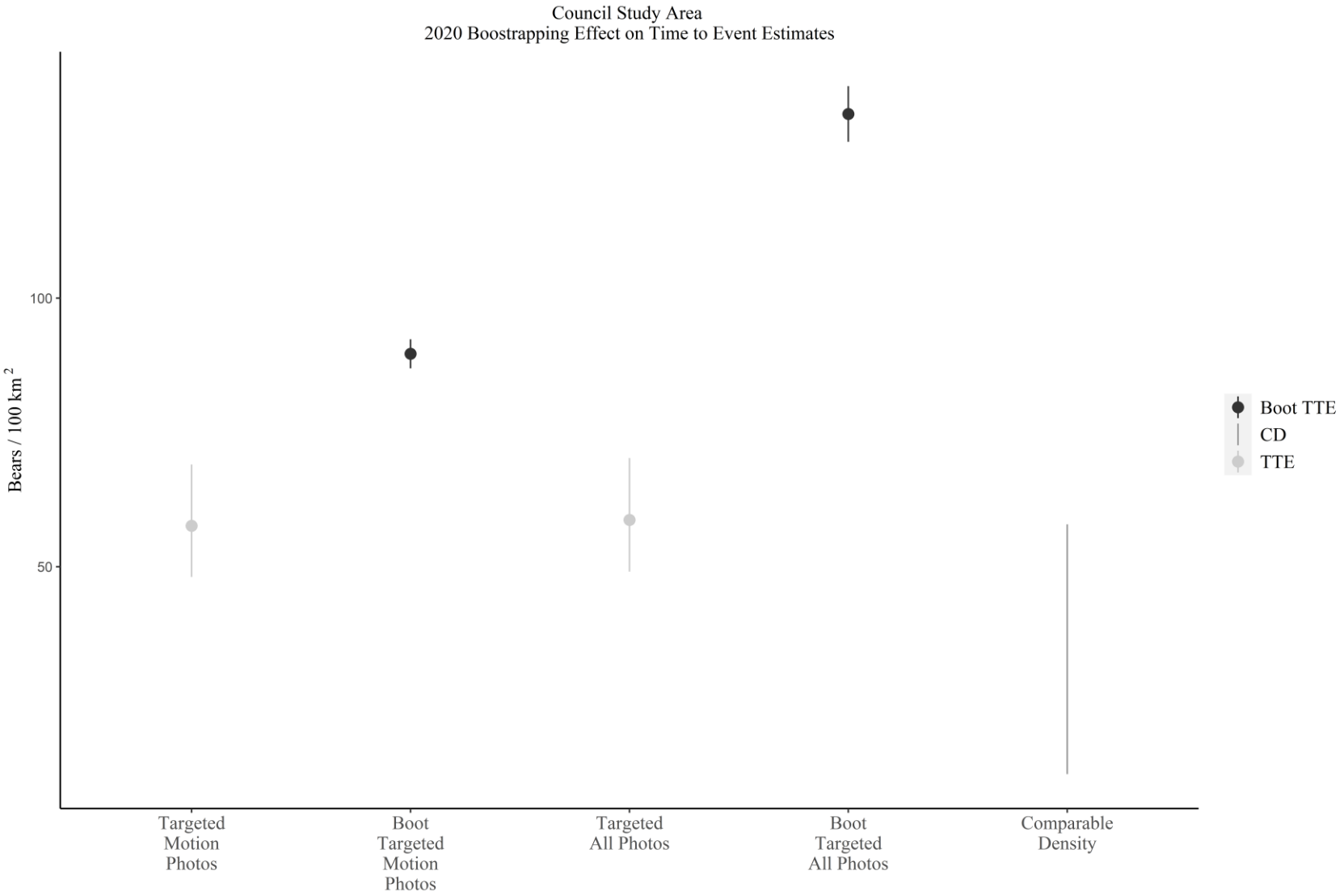

Figure A.6: The effect of bootstrapping on the time to event estimates in the Council study area (1,546 km^2), Idaho, USA, 2020.

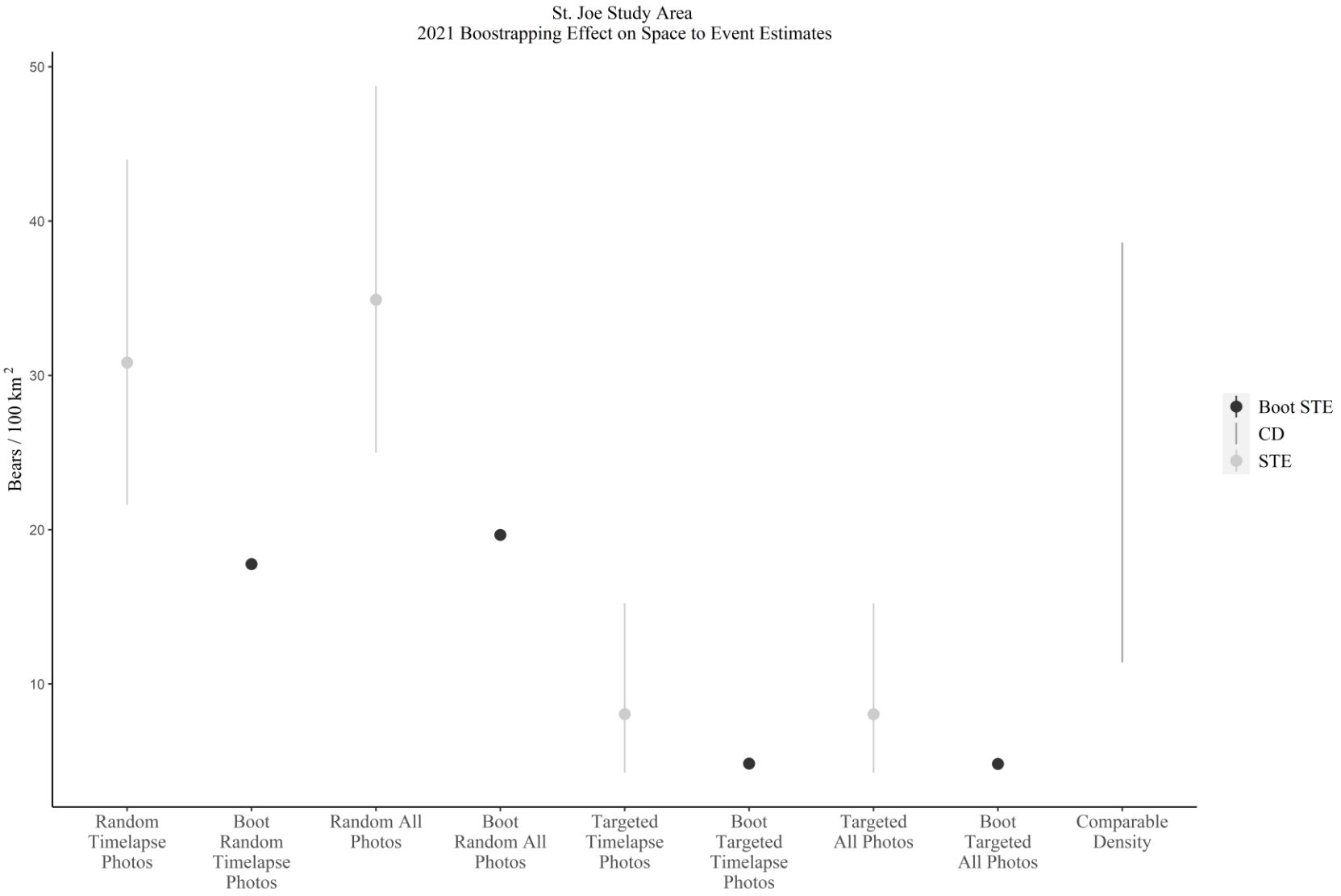

Figure A.7: The effect of bootstrapping on the space to event estimates in the St. Joe study area (2,727 km^2), Idaho, USA, 2021.

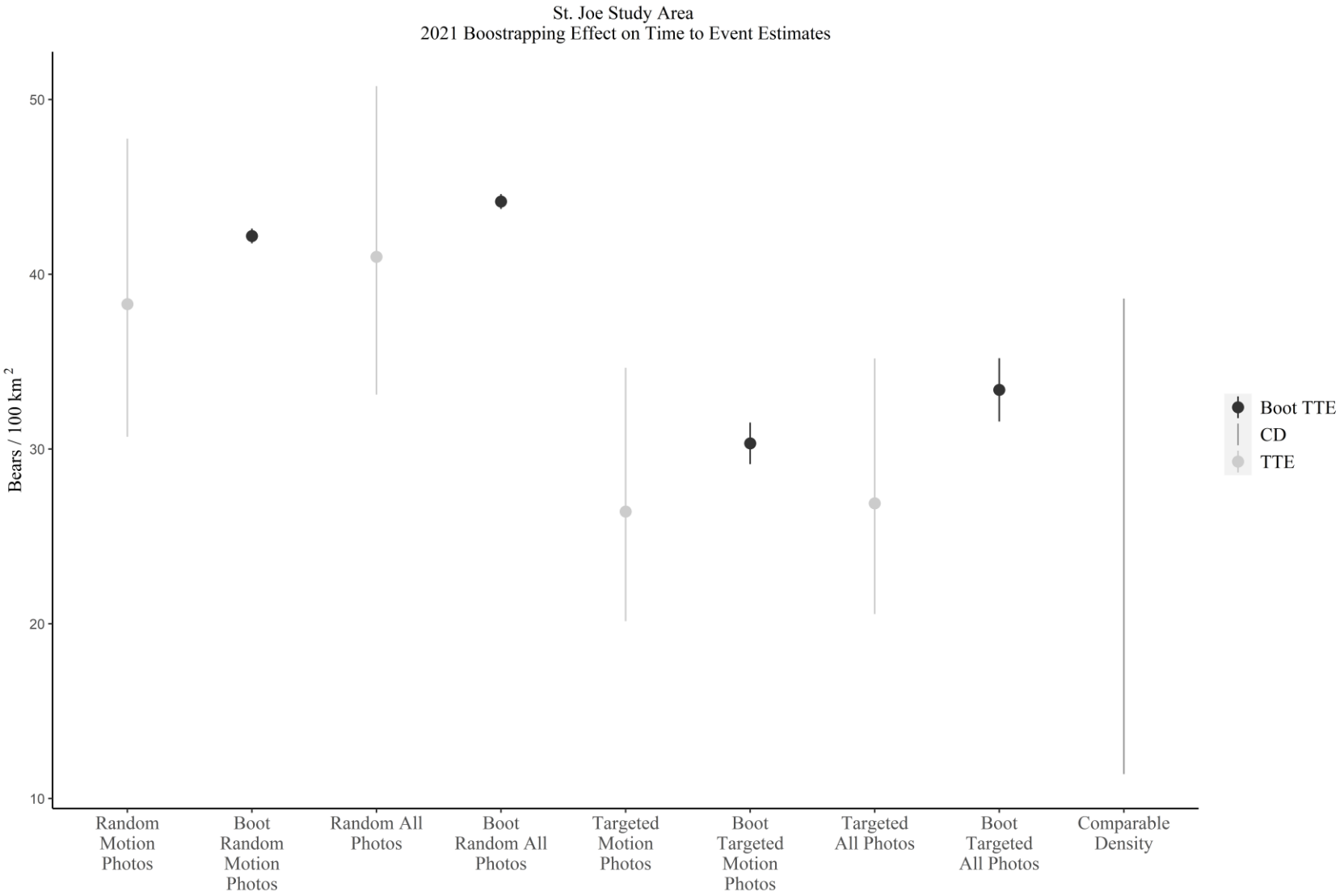

Figure A.8: The effect of bootstrapping on the time to event estimates in the St. Joe study area (2,727 km^2), Idaho, USA, 2021.

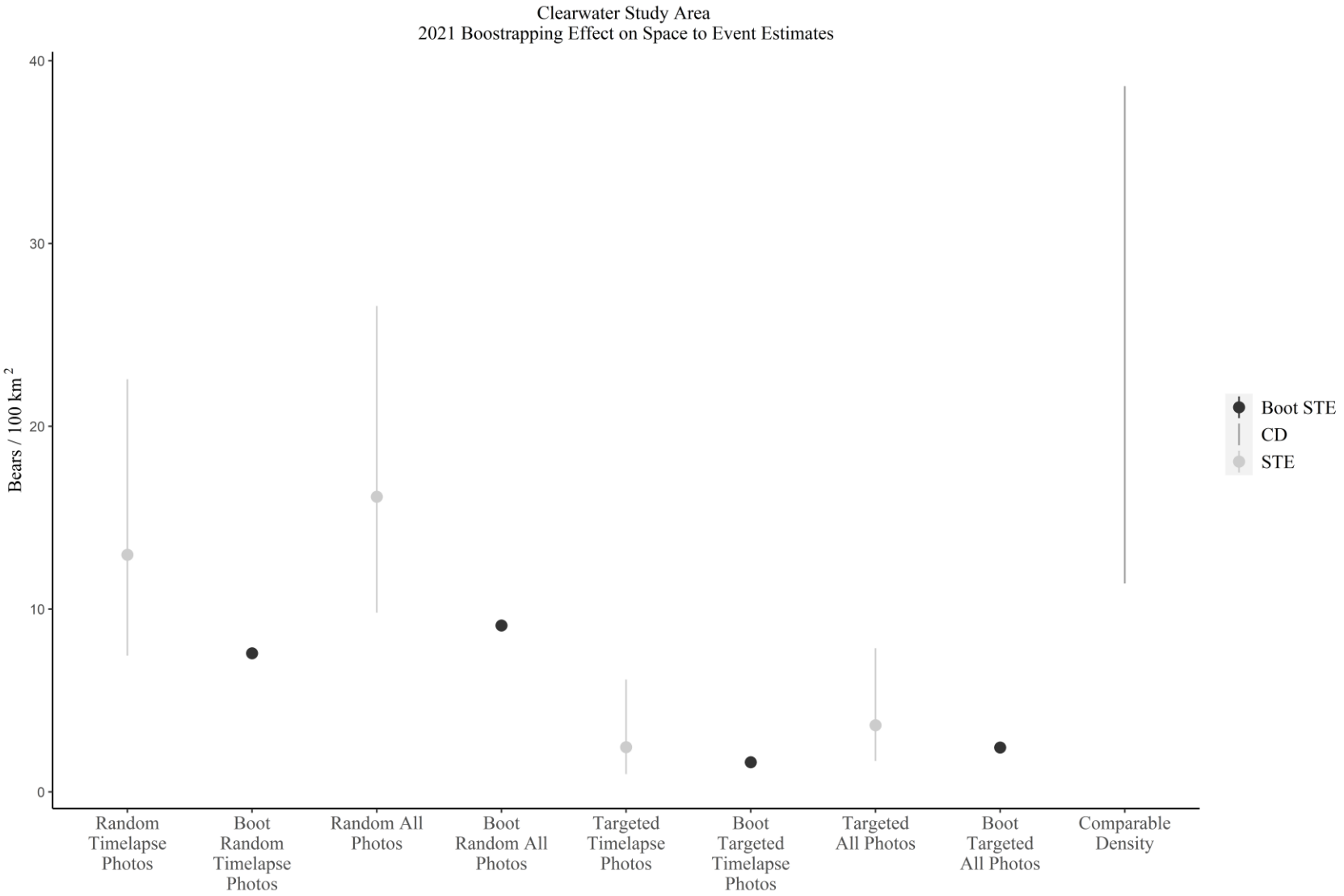

Figure A.9: The effect of bootstrapping on the space to event estimates in the Clearwater Study Area (4,029 km^2), Idaho, USA, 2021.

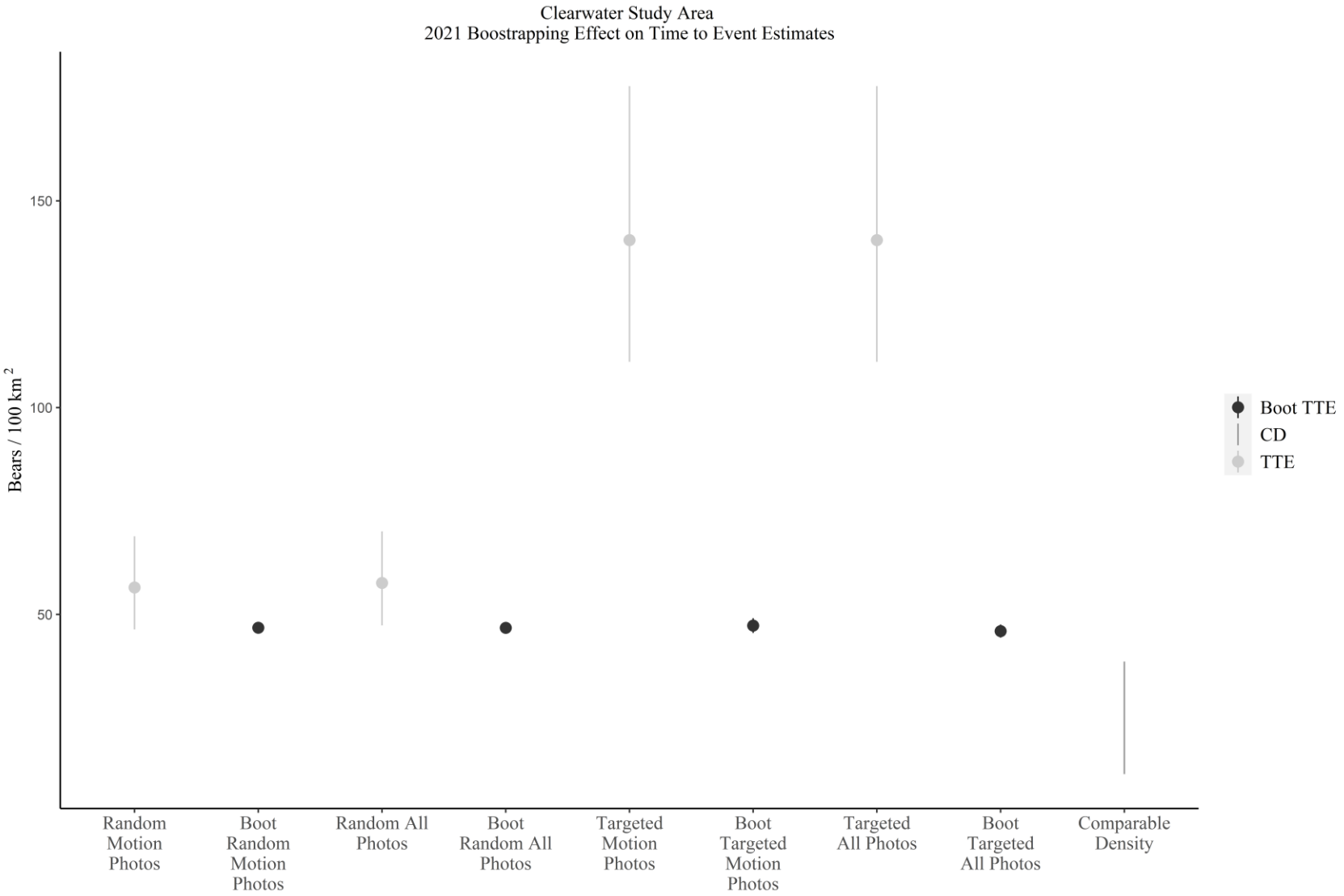

Figure A.10: The effect of bootstrapping on the time to event estimates in the Clearwater Study Area (4,029 km^2), Idaho, USA, 2021.

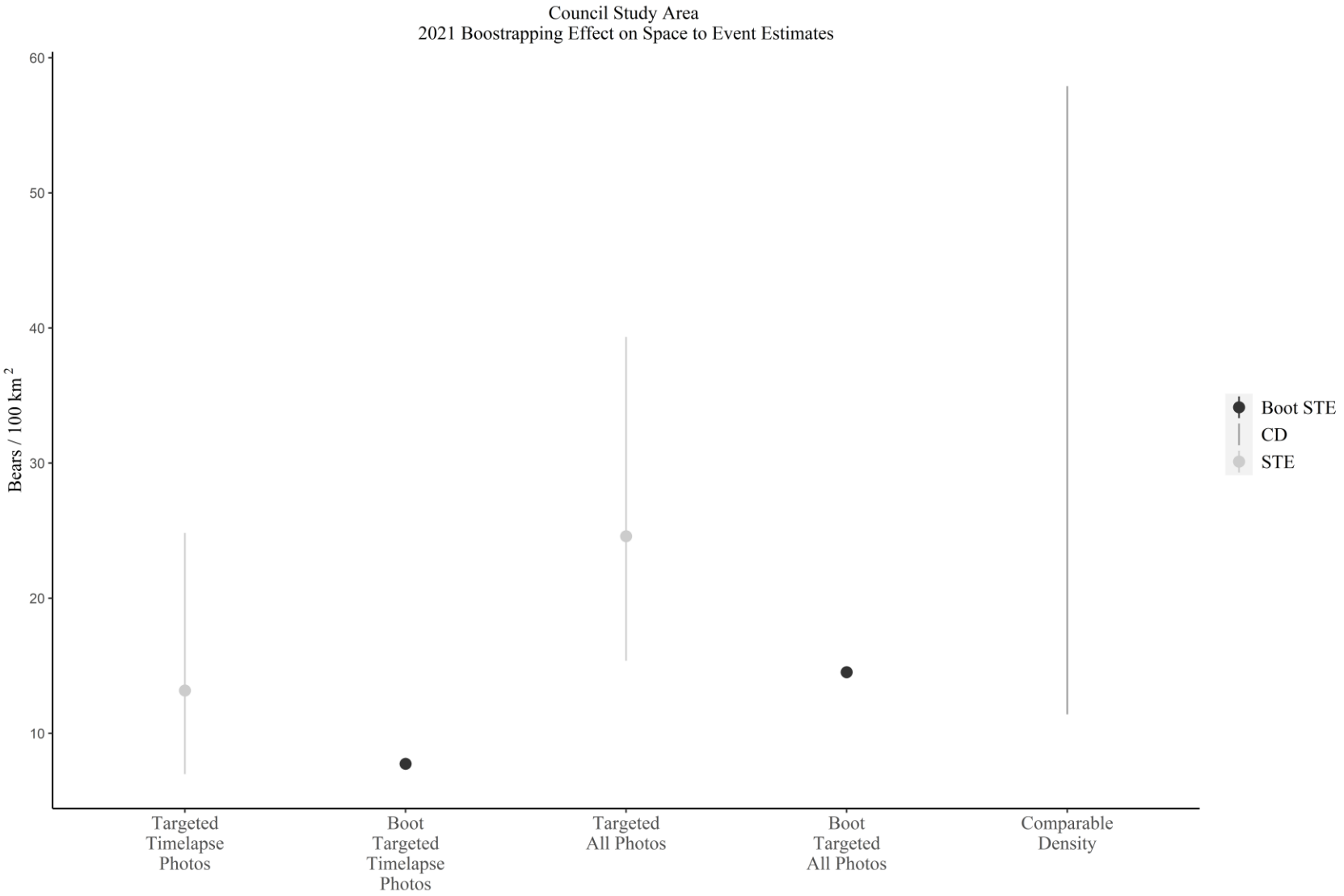

Figure A.11: The effect of bootstrapping on the space to event estimates in the Council study area (1,546 km^2), Idaho, USA, 2021.

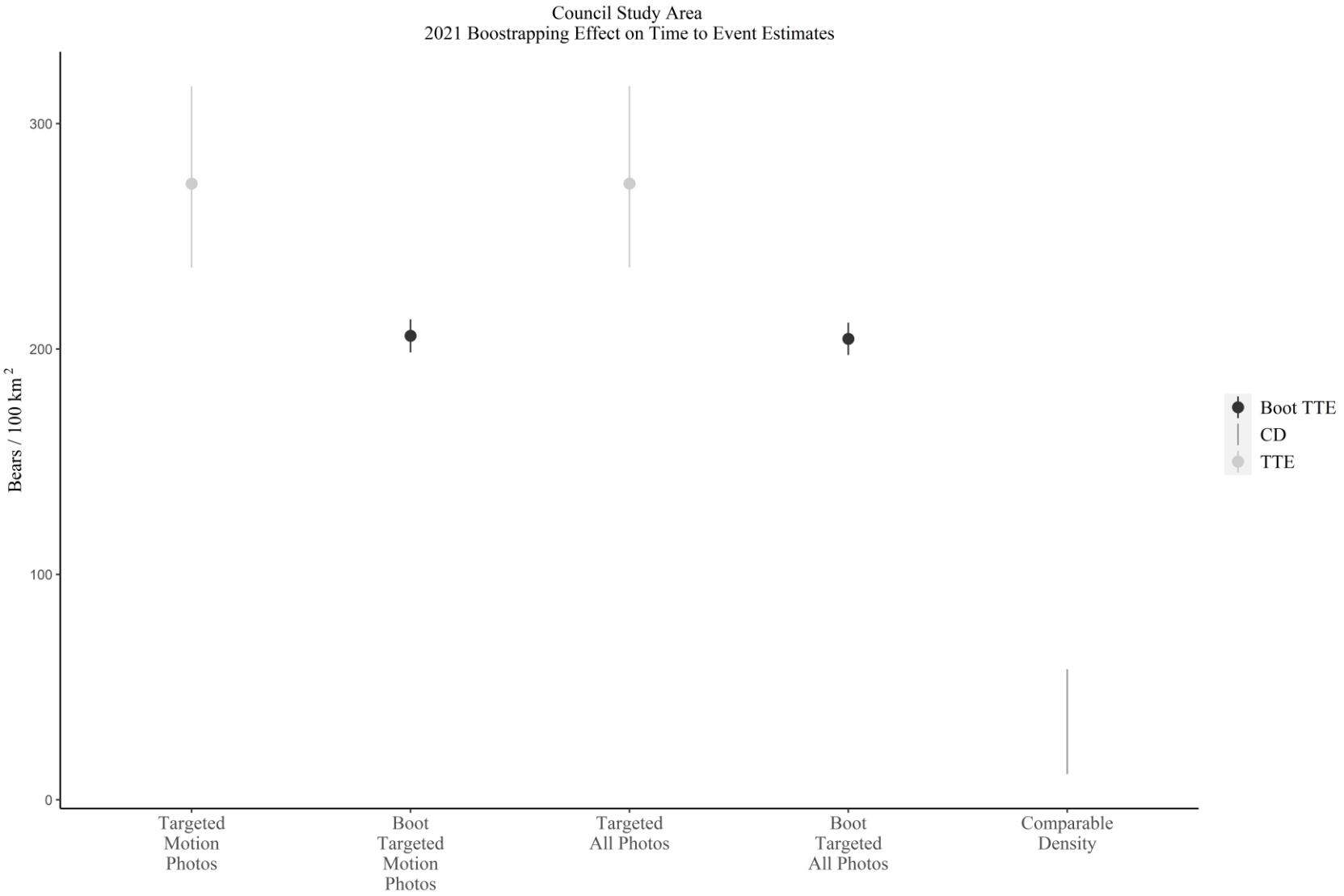

Figure A.12: The effect of bootstrapping on the time to event estimates in the Council study area (1,546 km^2), Idaho, USA, 2021.